R-1059

DAVIDSON LABORATORY

REPORT 1059

STEVENS INSTITUTE OF TECHNOLOGY

CASTLE POINT STATION
HOBOKEN, NEW JERSEY

AN ASPECT OF THE PROPELLER-SINGING PHENOMENON AS A SELF-EXCITED OSCILLATION

by

Jumpei Shioiri

March 1965

R-1059

DAVIDSON LABORATORY

Report 1059

March 1965

AN ASPECT OF THE PROPELLER-SINGING PHENOMENON AS A SELF-EXCITED OSCILLATION

by

Jumpei Shioiri

Sponsored by
Bureau of Ships General Hydromechanics
Research Program (S-R009-01-01)
Administered by David Taylor Model Basin
Contract Nonr 263(52)
(DL Project 2661/056)

Approved

Stavros Tsakonas

Stavros Tsakonas, Head
Fluid Dynamics Division

x and 35 pages
10 figures

ABSTRACT

A model for the propeller-singing phenomenon considered as a self-excited oscillation is presented to interpret the finding of a recent experimental work: viz., that, although the singing frequency roughly obeys the well-known Strouhal relation, once the strong singing state has been established, the frequency is kept constant through a fairly wide range of flow velocity, and consequently the frequency-versus-velocity diagram exhibits step and jump characteristics. The model presented is a "closed loop" composed of a blade, as a mechanical-vibration system, and the Kármán vortex-shedding mechanism; the blade vibration controls the shedding mechanism, and the hydrodynamic reaction of shed vortices sustains the blade vibration. The control imposed by the blade vibration upon the vortex shedding actually implies the synchronization of the latter with the former. The model which simulates the vortex-shedding mechanism is essentially a simplified mathematical expression for the disintegration process of the vortex sheets shed from the separation points into the rows of discrete vortices. The stability criterion derived for the synchronized run of the shedding mechanism, together with the positive-work criterion imposed upon the phase relation between the blade vibration and the hydrodynamic reaction of the shed vortices, gives a reasonable interpretation for the step and jump characteristics.

KEYWORD

Propeller-Singing

TABLE OF CONTENTS

NOMENCLATURE

A	shape parameter in "influence" functions (Equation [10])
a	growth-rate parameter of vortices
B	form constant (Equation [10])
b	shape parameter in "influence" functions (Equation [10])
C	chord length
c	integration constant (Equation [20])
D	dimensionless velocity (Equation [39])
d	trailing-edge thickness of body
E	function of vortex-induced velocity (Equation [39])
F	function defined by Equation (31a)
F_b	amplitude of hydrodynamic reaction force on blade
f	function (Equation [26])
f_b	natural frequency of blade
f_k	shedding frequency of Kármán vortices
g(x)	mode shape of blade vibration (Equation [46])

H	unit step function
h	amplitude in blade-vibration mode shape
k	characteristic parameter in Hurwitz-Routh stability criterion (Equation [36])
n	order of iteration process for criteria of stable synchronization
q	constant = 1 or 2 (Equation [39])
$S_1(x)$, $S_2(x)$	"influence" function (see Equation [27])
S_t	Strouhal number = $f_k\ d/U_\infty$
$S = \omega d/U_\infty = 2\pi S_t$	non-dimensional frequency parameter of Kármán vortex at free-shedding state
$S' = \omega' d/U_\infty = 2\pi S_t'$	non-dimensional frequency parameter at synchronization state
t	= time
$U_{(.)}$	flow velocity at separation point
U_o, $U_{o(.)}$	steady component of flow velocity at separation point
U_w	velocity at which vorticity is flowed away
U_∞	flow velocity at infinity
$u_{(..)}$	velocity induced by point vortex at separation point (see Equations [1] to [4])
u_o, $u_{o(.)}$	periodic component amplitude of flow velocity at separation point

u_{oo}	neutral value of u_o (see Equation [33])
w	see Equation (52)
x, y	coordinates in z-plane
z	physical plane
α	phase relation between velocities u_v and u_o
α_o	neutral value of α (see Equation [33])
β	see Equation (52)
α', β'	constants in "influence" functions (Equation [10])
$\Gamma_{(.)}$	circulation of point vortex (see Equations [1] to [4])
$\Gamma_{(.)}(x,t)$	vorticity distribution in vortex sheet
Γ_o, $\Gamma_{o(.)}$	mean vorticity in vortex sheet
$\Gamma_{s(.)}$	shedding rate of vorticity from separation point
$\gamma_o(x)$, $\gamma_{o(.)}(x)$	perturbation amplitude of vorticity distribution in vortex sheet
ϵ	small number
ζ	transformed plane
ξ, η	coordinates of ζ-plane

θ	phase angle between flow velocity due to blade vibration and velocity of blade vibration at separation point
Φ	expression given by Equation (34)
φ	angular coordinate along blade chord (Equation [40])
X	expression given by Equation (26)
Ψ	expression given by Equation (34)
ω	angular frequency of free vortex shedding
ω'	angular frequency of vortex shedding at synchronization state = natural frequency of blade vibration

Subscripts

i	refers to imaginary part
ℓ	refers to lower separation point
r	refers to real part
u	refers to upper separation part
v	refers to flow velocity induced by blade vibration

INTRODUCTION

The propeller-singing phenomenon has for a long time been understood as a forced vibration of the blade due to the hydrodynamic reaction force of the Kármán vortices shed from the trailing edge.

Recently, however, an experimental study[1] revealed a particular feature of the phenomenon: though the relation of singing frequency versus flow velocity roughly obeys the well-known Strouhal relation $f_k = S_t \frac{U_\infty}{d}$, the frequency in the strong singing state is nearly constant through a fairly wide range of flow velocity and consequently (as is shown in Figure 1) the relation of singing frequency versus flow velocity has steps.

Here

f_k = shedding frequency of the Kármán vortices

S_t = Strouhal number

U_∞ = flow velocity

d = trailing-edge thickness of body

Each frequency at strong singing state (characterized by a step) seems to correspond to one of the natural frequencies of the blade. During changes in the flow velocity, a strong singing state appears on each step, and successive changes cause the jump phenomena shown by the dotted lines in the figure. This kind of phenomenon was also observed in the experiment on suspension-bridge oscillation due to vortex shedding.[2]

Arnold et al[3] interpreted this particular feature of the strong-singing phenomenon as a special kind of resonance based on an experimental hypothesis that the shedding frequency of the Kármán vortices becomes lower with increase in amplitude of blade vibration. However, as is suggested by Krivstov and Pernik,[1] it is more natural to regard the singing phenomenon as a self-excited oscillation of the system which includes the Kármán vortices-shedding mechanism. In this paper, a model for the singing propeller is presented along this line.

SELF-EXCITED OSCILLATION LOOP FOR SINGING PHENOMENON

It is well known that the self-excited oscillation system is simulated by a "closed loop." For the propeller-singing phenomenon, the loop will be expressed as is shown in Figure 2. The "blade" element may be regarded essentially as a mechanical-vibration system. The other element — the Kármán vortices-shedding mechanism — is, on the other hand, a self-excited system which can continue to shed vortices periodically without any periodic stimulation from outside. This element plays the more important role in the singing phenomenon. The discrete structure of the Kármán vortices indicates that this self-excited system should have strong non-linear characteristics. The important aspect of such a non-linear self-excited system is the phenomenon called "synchronization" or "entrainment";[4] that is, the operation of the non-linear self-excited system is often synchronized with the periodic stimulation from outside which has a frequency not so different from the natural frequency of the system. In the present problem the above-mentioned phenomenon corresponds to the synchronization of shed vortices with blade vibration.

The blade element is, as stated above, essentially a mechanical-vibration system with large mass and stiffness, and definite natural frequencies f_b. The natural frequency of the Kármán vortices-shedding mechanism, given in the form $f_k = S_t \frac{U_\infty}{d}$, depends strongly upon the flow velocity U_∞. In the range of U_∞ in which f_k differs largely from the natural frequency of the blade f_b, the vibration amplitude of the blade due to the reaction force of the Kármán vortices will be small, and the signal from the blade element will be too weak to synchronize the Kármán vortices-shedding mechanism. In this condition, the loop in Figure 2 is open between these two elements, and the system is in the state of a mere forced vibration caused by the reaction of the shed vortices. This is the weak singing which occurs at the frequency corresponding to the Strouhal relation. When U_∞ is changed and f_k approaches f_b, the amplitude of the blade vibration becomes large enough — in other words, the signal from the blade element becomes strong enough — to synchronize the shedding of the vortices. Thus, the loop in Figure 2 is built up and the system enters into the strong active state. Of course, in this picture, it is necessary that the loop transfer function have unstable character. If the shedding mechanism of the vortices can be synchronized with the vibration of the blade through a fairly wide range of velocity, one can see that, with the strong singing state established, frequency remains constant at one of the natural frequencies of the blade, through a certain flow-velocity range.

The strong singing state of the present model will occur when the Kármán vortices-shedding mechanism is synchronized with the blade vibration and, furthermore, when a favorable phase relation between the blade vibration and the hydrodynamic reaction exists. If these conditions are lost by changing the flow velocity, the system will jump from the strong singing state to a weak singing one with constant Strouhal number and will continue in the latter state until it reaches the next natural frequency, where another cycle of strong singing will appear.

THE KÁRMÁN VORTICES SHEDDING MECHANISM AND ITS SYNCHRONIZATION WITH BLADE VIBRATION

To provide concrete support for the above discussion, a suitable model for the vortices-shedding mechanism should be presented. Von Kármán's work notes the stability of the vortex rows, but it does not explain how these rows of discrete vortices come into existence. This, together with the fact that we lack any record of experimental observations of the flow near the trailing edge and in the wake of an oscillating body, proves a stumbling block in the present analysis. A mathematical model will be presented here which possesses the synchronization mechanism and the main features of the above-mentioned propeller-singing phenomenon.

PRESENTATION OF THE MODEL

The vortex-shedding process may be dealt with by solving the Navier-Stokes equation under given conditions. The analytical approach, however, seems desperate, and the numerical attack also seems hopeless (except for the case of low Reynolds number) even if a computer with large capacity is used. Another approach may be to treat the process as a kind of Helmholtz instability problem[5] (using the method adopted by Rosenhead[6]), since observation of the downstream flow of a body with a blunt trailing shape indicates that the vortex sheets, which originate from the vorticity in the boundary layers and are shed from the separation points, roll up and concentrate into rows of discrete vortices a rather short distance away. The model presented here is constructed on the basis of this description, with some speculative mathematical simplifications which are adopted in order to introduce a non-linear oscillation version into the field of hydrodynamics and to obtain a wider view of the particular feature of the singing phenomenon described in the previous sections of this report.

As noted earlier, the vortex-shedding mechanism is a self-excited system and itself should have a closed loop, which plays the role of a "minor loop" in the main loop shown in Figure 2. On the basis of the foregoing description, the synthesis of the loop of the shedding mechanism may be given as follows:

(1) The existing downstream vortex rows exert a periodic flow disturbance upon the separation points.

(2) This flow disturbance at the separation points causes a periodic disturbance in the strengths of the vortices which are shed from the separation points into the vortex sheets.

(3) Thus the generated non-uniformity of the vorticity distribution in the vortex sheets plays the role of the embryo of the discrete vortices; or, in other words, this non-uniformity grows up into the Kármán vortex streets.

The block diagram of the thus synthesized loop and the corresponding schematic picture of the flow are shown in Figure 3.

If the blade is vibrating, flow disturbance due to the vibration may be superimposed on that due to the shed vortices at the separation points, as is shown in the block diagram of Figure 3 by a dotted line. This flow disturbance due to blade vibration plays the role of the synchronization trigger signal.

MATHEMATICAL EXPRESSION FOR THE CONSTITUENT ELEMENTS

Assuming two-dimensional ideal-fluid flow, the mathematical expression of the constituent elements for the foregoing model may be given as follows:

(a) The Disturbance Velocity at the Separation Points Induced by the Downstream Vortices

The velocities induced by the shed vortices at the separation points are affected by the shape of the body. For simplicity, let us consider first a circular cylinder body of unit radius. The coordinate system is shown in Figure 4a. It is assumed that the flow separation points are located at ($x = 0$, $y = \pm 1$) and that the vortices shed from the separation points are flowed away along the lines $y = \pm 1$. The induced velocity $U_{uu}(x)$ of an isolated vortex Γ_u located at $(x = x,\ y = +1)$ and of its corresponding image (as shown in Figure 4a) upon the upper separation point $(x = 0,\ y = +1)$ is given as

$$u_{uu}(x) = -\frac{\Gamma_u}{2\pi} \tag{1}$$

Similarly, the effect of Γ_ℓ at $(x = x,\ y = -1)$ and of its corresponding image upon the upper separation point is

$$u_{u\ell}(x) = -\frac{\Gamma_\ell}{2\pi}\left(1 - \frac{2^2}{x^2 + 2^2}\right) \tag{2}$$

In the same way, the effects of Γ_u and Γ_ℓ upon the lower separation points are given by

$$u_{\ell u}(x) = \frac{\Gamma_u}{2\pi}\left(1 - \frac{2^2}{x^2 + 2^2}\right) \tag{3}$$

$$u_{\ell\ell}(x) = \frac{\Gamma_\ell}{2\pi} \tag{4}$$

The functions $S_{uu}(x)$, $S_{u\ell}(x)$, $S_{\ell u}(x)$, and $S_{\ell\ell}(x)$ are introduced, and we have

$$S_{uu}(x) = \frac{u_{uu}(x)}{\Gamma_u} \qquad S_{u\ell}(x) = \frac{u_{u\ell}(x)}{\Gamma_\ell}$$

$$S_{\ell u}(x) = \frac{u_{\ell u}(x)}{\Gamma_u} \qquad S_{\ell\ell}(x) = \frac{u_{\ell\ell}(x)}{\Gamma_\ell} \tag{5}$$

For convenience, these are called "influence functions," since they represent the effects of the unit strength vortex at $(x = x,\ y = \pm 1)$ on the induced velocity at the separation points. These functions are graphically exhibited in Figure 4b.

In the case of a body with trailing edge of parabolic shape (Figure 5a) given by

$$y^2 = 1 - (2/3)\,x \tag{6}$$

with flow separation points at $x = 0$, $y = \pm 1$, it is assumed that the shed vortices are flowed away along the lines

$$y = \pm \frac{1}{3}\left(2 + \frac{1}{x+1}\right)$$

which are tangential to the body surface at the separation points.

The conformal transformation

$$\zeta = \sqrt{z - \frac{4}{3}} - \sqrt{\frac{1}{6}} \tag{7}$$

which maps the flow field in the z-plane into the right half of the ζ-plane (Figure 5b), provided that a cut along the x-axis from $-\infty$ to 4/3 is introduced, determines the complex velocity potential by means of the "wall effect." The influence functions $S_{uu}(x)$, $S_{u\ell}(x)$, $S_{\ell u}(x)$, $S_{\ell\ell}(x)$ are evaluated and exhibited in Figure 5c. The influence functions for both circular cylinder body and parabolic trailing-edge body exhibit the following general features, as shown by Figures 4b and 5c:

(1) $$S_{uu}(x) = - S_{\ell\ell}(x)$$
$$S_{u\ell}(x) = - S_{\ell u}(x) \tag{8}$$

(2) $S_{uu}(x)$ and $S_{\ell\ell}(x)$ have finite value at $x = 0$, while $S_{u\ell}(x)$ and $S_{\ell u}(x)$ are zero at $x = 0$. These functions have an incubation interval before a large rate of increase appears with increasing x , and remain almost constant at still larger x .

(3) For large values of x ,

$$S_{u\ell}(x) \sim S_{uu}(x) \quad \text{and} \quad S_{\ell u}(x) \sim S_{\ell\ell}(x) \tag{9}$$

By utilization of these general characteristic features, the influence function can be approximately expressed by

$$\begin{aligned} S_{uu}(x) &= - S_{\ell\ell}(x) = - Ae^{-\alpha' x} \\ S_{u\ell}(x) &= - S_{\ell u}(x) = \left(- Ae^{-\alpha' x} + Be^{-\beta' x}\right) H(b) \end{aligned} \tag{10}$$

where $H(b)$ is the unit step function at $x = b$ and A , B , α', and β' are positive constants.

For further simplification, the motivation of which will become apparent in the discussion which follows in a later section, it is assumed that $B = 0$, $\beta' = 0$, and $\alpha' \to 0$; hence

$$\begin{aligned} S_{uu}(x) &= - S_{\ell\ell}(x) = \lim_{\alpha' \to 0} \left(- Ae^{-\alpha' x}\right) \\ S_{u\ell}(x) &= - S_{\ell u}(x) = \lim_{\alpha' \to 0} \left[- Ae^{-\alpha' x} H(b)\right] \end{aligned} \tag{11}$$

This simplification affects the results quantitatively, but presumably not qualitatively.

(b) The Strength of Shed Vorticity in Terms of Flow Velocity at Separation Points

Let the velocity distribution in the boundary layer, the velocity outside the boundary layer, and the thickness of the boundary layer at the upper separation point be designated by $U_u(y)$, U_u , and δ , respectively. The vorticity shed per unit time from the upper separation point into the upper vortex sheet is given by

$$\Gamma_{su} = \int_0^{\delta} U_u(y) \frac{d\, U_u(y)}{dy}\, dy = \frac{1}{2} U_u^2 \tag{12}$$

Similarly, for the lower separation point,

$$\Gamma_{s\ell} = \frac{1}{2} U_\ell^2 \tag{12a}$$

where U_ℓ is the velocity outside the boundary layer at the lower separation point.

If it is assumed that the velocity at the upper separation point, U_u, is composed of the mean velocity U_{ou} and a small perturbation velocity of periodic nature, $u_{ou}e^{i\omega t}$, then the vorticity shedding rate from the upper separation point is given by

$$\Gamma_{su} \sim \frac{1}{2}\left(U_{ou}^2 + 2U_{ou}u_{ou}e^{i\omega t}\right) \tag{13}$$

and similarly from the lower separation point, by

$$\Gamma_{s\ell} \sim \frac{1}{2}\left(U_{o\ell}^2 + 2U_{o\ell}u_{o\ell}e^{i\omega t}\right) \tag{14}$$

(c) Concentrating Process, Vortex Sheets into Discrete Vortex Rows

Rosenhead's treatment[6] for the rolling-up phenomenon of the vortex sheet in the Helmholtz instability problem indicates that the local disturbance in the vorticity density in the vortex sheet causes a geometrical deformation of the sheet. This deformation gives rise to the migration of the vortices in a manner which promotes the growth of vorticity density; thus these two processes cooperate in causing an accelerating concentration of vorticity. In the present treatment, a simple mathematical expression, based on the above-mentioned feature of the Helmholtz instability problem, is given for the disintegration process involving the shedding of the vortex sheets from the separation points into discrete vortex rows.

It is assumed that the process follows the pattern outlined below and shown in Figure 6.

(1) The vortex sheets shed from the separation points are flowed

away along the designated path.

(2) The vorticity densities in the sheets have sinusoidal disturbances due to the periodic fluctuations in the vorticity-shedding rate given by Equations (13) and (14).

(3) The amplitudes of the disturbances increase with distance x from the separation points.

According to this picture the vorticity distributions in the upper and the lower sheets may be expressed as

$$\Gamma_u(x,t) = \Gamma_{ou} + \gamma_u(x,t) = \Gamma_{ou} + \gamma_{ou}(x)e^{i\omega[t - (x/U_w)]}$$

and (15)

$$\Gamma_\ell(x,t) = \Gamma_{o\ell} + \gamma_\ell(x,t) = \Gamma_{o\ell} + \gamma_{o\ell}(x)e^{i\omega[t - (x/U_w)]}$$

respectively, where U_w is the constant velocity in the x-direction by which the vorticity is flowed away, Γ_{ou} and $\Gamma_{o\ell}$ are the mean vorticity densities in the sheets, and $\gamma_{ou}(x)$ and $\gamma_{o\ell}(x)$ are the amplitudes of the disturbance terms in the vorticity densities. On the basis of the continuity equation

$$\Gamma_{su}\Delta t = \Gamma_u U_w \Delta t$$

where Δt is a specified interval of time, together with Equations (13) and (14), it is apparent that

$$\Gamma_{ou} = \frac{1}{2}\,\frac{U_{ou}^2}{U_w} \qquad \gamma_{ou}(0) = \frac{U_{ou}u_{ou}}{U_w} \tag{16}$$

and

$$\Gamma_{o\ell} = \frac{-1}{2}\,\frac{U_{o\ell}^2}{U_w} \qquad \gamma_{o\ell}(0) = \frac{-U_{o\ell}u_{o\ell}}{U_w} \tag{17}$$

It will be assumed that the process which embraces the passing of the vortices from the embryonic stage to complete disintegration into discrete vortices is completed at the stage where the amplitude of the perturbation vorticity density becomes equal to the mean vorticity strength of the sheet.

The simplest mathematical expression which satisfies the above requirement and fixes the growing rate with x of the disturbance amplitudes $|\gamma_{ou}(x)|$ and $|\gamma_{o\ell}(x)|$ is assumed to be

$$\frac{d}{dx}\left(\frac{|\gamma_o(x)|}{|\Gamma_o|}\right) = a\,\frac{|\gamma_o(x)|}{|\Gamma_o|}\left(1 - \frac{|\gamma_o(x)|}{|\Gamma_o|}\right) \tag{18}$$

where the constant a is the growth-rate parameter. The absolute value has been introduced so that the above relation will hold true for either upper or lower vortex sheet. It is obvious that this relation ensures the final value of $|\gamma_o(x)|$ as equal to $|\Gamma_o|$.

The solution is given by

$$\frac{|\gamma_o(x)|}{|\Gamma_o|} = \frac{e^{ax+c}}{1+e^{ax+c}} \tag{19}$$

where the constant c is

$$c = \ell n\left[\frac{|\gamma_o(o)/\Gamma_o|}{1 - |\gamma_o(o)/\Gamma_o|}\right] \tag{20}$$

The value of $\gamma_o(x)/|\Gamma_o|$ is graphically exhibited (see dotted lines) in Figure 7, in terms of $ax + c$. If for simplicity the value of $|\gamma_o(x)|/|\Gamma_o|$ is replaced by a unit step function at $ax + c = 0$, then it can be seen (from Figure 7) that a suitable approximation of the function $|\gamma_o(x)|/|\Gamma_o|$ is obtained. Hence

$$\frac{|\gamma_o(x)|}{|\Gamma_o|} = H\left\{\frac{1}{a}\,\ell n\left[\frac{1 - |\gamma_o(o)/\Gamma_o|}{|\gamma_o(o)/\Gamma_o|}\right]\right\} \tag{21}$$

where $H(x)$ denotes a unit step function at x. Applying Equation (21) to Equations (15), (16), and (17), the vorticity distribution on the upper and lower vortex sheets will be given by

$$\Gamma_u(x\cdot t) = \frac{1}{2}\frac{U^2_{ou}}{U_w}\left\{1 + \frac{u_{ou}}{|u_{ou}|} H\left[\frac{1}{a}\ \ell n\left(\frac{1 - 2|u_{ou}|/U_{ou}}{2|u_{ou}|/U_{ou}}\right)\right]e^{i\omega(t-x/U_w)}\right\}$$

and

$$\Gamma_\ell(x\cdot t) = -\frac{1}{2}\frac{U^2_{o\ell}}{U_w}\left\{1 + \frac{u_{o\ell}}{|u_{o\ell}|} H\left[\frac{1}{a}\ \ell n\left(\frac{1 - 2|u_{o\ell}|/U_{o\ell}}{2|u_{o\ell}|/U_{o\ell}}\right)\right]e^{i\omega(t-x/U_w)}\right\} \quad (22)$$

where

$$U_u = U_{ou} + u_{ou}e^{i\omega t}$$

and

$$U_\ell = U_{o\ell} + u_{o\ell}e^{i\omega t}$$

are the velocities at upper and lower separation points respectively.

FREE SHEDDING OF THE KÁRMÁN VORTICES

Now it is possible to compose a mathematical equation for the closed loop of the vortices-shedding mechanism. The closed-loop equations with respect to the upper and the lower separation points are

$$U_u - U_\infty = \int_o^\infty \left[S_{uu}(x)\ \Gamma_u(x,t) + S_{u\ell}(x)\ \Gamma_\ell(x,t)\right] dx$$

$$U_\ell - U_\infty = \int_o^\infty \left[S_{\ell\ell}(x)\ \Gamma_\ell(x,t) + S_{\ell u}(x)\ \Gamma_u(x,t)\right] dx \quad (23)$$

where U_∞ denotes the uniform flow velocity at infinity and the other notations are as given in Equations (9) and (10).

Here, the following assumptions are introduced:

(a) $$\gamma_{ou}(x) = \gamma_{o\ell}(x) \qquad (24)$$

Therefore, from Equations (16) and (17),

$$u_{ou} = - u_{o\ell}$$

As can be seen in Figure 6, this assumption is imposed by the well-known arrangement of vortices typical to the Kármán vortex street.

(b) $$U_{ou} = U_{o\ell} = U_\infty = 2U_w \qquad (25)$$

If the body is flat in the direction of the main flow, and if the wake region near the trailing edge is regarded as dead water, the relations of Equation (25) should give a good approximation.

Then Equation (23), together with Equation (22), yields the time-dependent part of the shedding mechanism:

$$\frac{u_{ou}e^{i\omega t}}{U_\infty} = \int_0^\infty \left\{ S_{uu}(x) \frac{u_{ou}}{|u_{ou}|} H\left[\frac{1}{a} f\left(\frac{2|u_{ou}|}{U_\infty}\right)\right] - S_{u\ell}(x) \frac{u_{o\ell}}{|u_{o\ell}|} H\left[\frac{1}{a} f\left(\frac{2|u_{o\ell}|}{U_\infty}\right)\right]\right\} \cdot e^{i\omega(t-2x/U_\infty)}\, dx$$

$$\frac{u_{o\ell}e^{i\omega t}}{U_\infty} = \int_0^\infty \left\{ -S_{\ell\ell}(x) \frac{u_{o\ell}}{|u_{o\ell}|} H\left[\frac{1}{a} f\left(\frac{2|u_{o\ell}|}{U_\infty}\right)\right] + S_{\ell u}(x) \frac{u_{ou}}{|u_{ou}|} H\left[\frac{1}{a} f\left(\frac{2|u_{ou}|}{U_\infty}\right)\right]\right\} \cdot e^{i\omega(t-2x/U_\infty)}\, dx$$

where

$$f(x) = \ell n \left(\frac{1-x}{x}\right) \quad \text{and} \quad x = \frac{2u_{ou,\ell}}{U_\infty} \qquad (26)$$

If the symmetrical relations, Equations (8) and (24), are taken into account, the two equations in Equation (26) become identical and can be expressed as

$$\frac{u_o}{U_\infty} = \int_o^\infty \left[S_1(x) + S_2(x)\right] H\left[\frac{1}{a} f\left(\frac{2u_o}{U_\infty}\right)\right] e^{-iSx}\, dx \tag{27}$$

where

$$u_o = u_{ou} = -u_{o\ell}$$

$$S_1(x) = S_{uu}(x) = -S_{\ell\ell}(x) = \lim_{\alpha'\to o} \left(-Ae^{-\alpha' x}\right)$$

$$S_2(x) = S_{u\ell}(x) = -S_{\ell u}(x) = \lim_{\alpha'\to o} \left[-Ae^{-\alpha' x} H(b)\right]$$

$$S = 2\omega/U_\infty$$

If the representative thickness of the body is taken as 2 (the value taken as the separation-point thickness) in the evaluation of $S_1(x)$ and $S_2(x)$, then

$$S = 2\pi S_t \tag{28}$$

where S_t is the Strouhal number.

It should be noted that, due to the symmetry relations introduced by Equations (8), (24), and (25), the system of simultaneous equations given by Equation (23) or (26) for the upper and lower separation points is reduced to a single equation (Equation [27]).

Upon integration, Equation (27) yields

$$\frac{u_o}{U_\infty} = iA\frac{1}{S}\left[e^{-iS\frac{1}{a} f\left(\frac{2u_o}{U_\infty}\right)} + e^{-iSb}\right]$$

$$\text{for} \quad b > \frac{1}{a} f\left(\frac{2u_o}{U_\infty}\right) \tag{29}$$

or

$$\frac{u_o}{U_\infty} = iA\frac{1}{S}\left[2e^{-iS\frac{1}{a}f\left(\frac{2u_o}{U_\infty}\right)}\right]$$

$$\text{for} \quad b < \frac{1}{a}f\left(\frac{2u_o}{U_\infty}\right)$$

The real and imaginary parts of the above expressions are sufficient to determine the unknown S and $\frac{u_o}{U_\infty}$.

SYNCHRONIZATION OF SHEDDING MECHANISM WITH BLADE VIBRATION — STABILITY CRITERIA

If the blade vibration induces periodic flow disturbances $u_{vu}e^{i\omega' t}$ and $u_{v\ell}e^{i\omega' t}$ at the upper and the lower separation points respectively, these may act as a synchronization signal, as is shown in the block diagram of Figure 3. Assuming the symmetrical relation

$$u_{vu} = -u_{v\ell}(= u_v) \tag{30}$$

the loop equation for the synchronized condition is obtained as

$$\frac{u_o}{U_\infty}e^{i\alpha} = e^{i\alpha}\int_0^\infty \left[S_1(x) + S_2(x)\right] H\left[\frac{1}{a}f\left(\frac{2u_o}{U_\infty}\right)\right] e^{-iS'x}\,dx + \frac{u_v}{U_\infty} \tag{31}$$

where

$$S' = \omega'\frac{2}{U_\infty}$$

and α is the phase relation between u_v and u_o.

It should be noted that in the above equation the periodic disturbance induced by the blade vibration is assumed to be known, whereas the total perturbation velocity at the separation point, u_o, and the phase angle α are both unknown and will be determined by the solution of Equation (31). It should be pointed out, also, that Equation (31) describes the neutral condition for the synchronization, and that there is thus a possibility that its solution will represent the unstable synchronization state, where small deviations from the neutral condition may grow unboundedly with increasing time. To exclude this possibility, a stability analysis for the synchronization must be performed. The powerful method introduced by Van del Pol for stability analysis[7] cannot be utilized in the present case, since Equation (31) is an algebraic equation stating simply the neutral condition; hence the timewise growth and decay of any deviation from this condition is not taken into account. In this paper, the following approximate method will be used.

An iteration scheme is developed based on the fact that the n^{th} iterative values of u_o and α, written in the form

$$u_o = u_{oo} + (\Delta u_o)_n$$

$$\alpha = \alpha_o + (\Delta\alpha)_n$$

can be obtained from their (n-1)th values,

$$u_o = u_{oo} + (\Delta u_o)_{n-1}$$

and

$$\alpha = \alpha_o + (\Delta\alpha)_{n-1}$$

(where u_{oo} and α_o are the values at the neutral condition and Δu_o and $\Delta\alpha$ are small deviations from these values) by means of Equation (31). Let

$$F\left[f\left(\frac{2u_o}{U_\infty}\right)\right] = \int_0^\infty \left[S_1(x) + S_2(x)\right] H\left[\frac{1}{a} f\left(\frac{2u_o}{U_\infty}\right)\right] e^{-iS'x}\, dx$$

Then Equation (31) can be written as

$$\frac{u_o}{U_\infty} e^{i\alpha} = e^{i\alpha} F\left[f\left(\frac{2u_o}{U_\infty}\right)\right] + \frac{u_v}{U_\infty} \tag{31a}$$

Substitution of the n^{th} iterative values on the left-hand side and the (n-1)th values on the right-hand side of this equation yields

$$\frac{u_{oo} + (\Delta u_o)_n}{U_\infty} e^{i\left[\alpha_o + (\Delta\alpha)_n\right]} = e^{i\left[\alpha_o + (\Delta\alpha)_{n-1}\right]} F\left\{ f\left[\frac{2}{U_\infty}\left(u_{oo} + \{\Delta u_o\}_{n-1}\right)\right]\right\} + \frac{u_v}{U_\infty}$$

If only the zero- and first-order terms are kept in this iteration scheme, the following approximate equation results:

$$\frac{u_{oo}}{U_\infty} e^{i\alpha_o} + \frac{(\Delta u_o)_n}{U_\infty} e^{i\alpha_o} + i\,\frac{u_{oo}}{U_\infty}(\Delta\alpha)_n\, e^{i\alpha_o}$$

$$\approx F\left[f\left(\frac{2u_{oo}}{U_\infty}\right)\right] e^{i\alpha_o} + iF\left[f\left(\frac{2u_{oo}}{U_\infty}\right)\right](\Delta\alpha)_{n-1}\, e^{i\alpha_o}$$

$$+ \left(\frac{dF}{df}\frac{df}{du_o}\right)_{u_o = u_{oo}} (\Delta u_o)_{n-1}\, e^{i\alpha_o} + \frac{u_v}{U_\infty} \tag{32}$$

From Equation (31a), at the neutral condition,

$$\frac{u_{oo}}{U_\infty} e^{i\alpha_o} = e^{i\alpha_o} F\left[f\left(\frac{2u_{oo}}{U_\infty}\right)\right] + \frac{u_v}{U_\infty} \tag{33}$$

Substitution of Equation (33) into Equation (32) yields

$$\frac{(\Delta u_o)_n}{U_\infty} + i\,\frac{u_{oo}}{U_\infty}(\Delta\alpha)_n = \left(\frac{dF}{df}\frac{df}{du_o}\right)_{u_o = u_{oo}} (\Delta u_o)_{n-1} + iF\left[f\left(\frac{2u_{oo}}{U_\infty}\right)\right] (\Delta\alpha)_{n-1}$$

Subtracting

$$\frac{(\Delta u_o)_{n-1}}{U_\infty} + i\,\frac{u_{oo}}{U_\infty}(\Delta\alpha)_{n-1}$$

from both sides of the foregoing equation results in

$$\frac{(\Delta u_o)_n - (\Delta u_o)_{n-1}}{U_\infty} + i \frac{u_{oo}}{U_\infty}\left[(\Delta\alpha)_n - (\Delta\alpha)_{n-1}\right]$$

$$= \Psi \frac{(\Delta u_o)_{n-1}}{U_\infty} + \Phi \frac{u_{oo}}{U_\infty}(\Delta\alpha)_{n-1} \tag{34}$$

where

$$\Psi = \left\{\left[\frac{dF}{df}\frac{df}{du_o}\right]_{u_o = u_{oo}} - \frac{1}{U_\infty}\right\} U_\infty$$

$$\Phi = i\left\{\left[F\right]_{u_o = u_{oo}} - \frac{u_{oo}}{U_\infty}\right\}\frac{U_\infty}{u_{oo}}$$

Since $(\Delta u_o)_n - (\Delta u_o)_{n-1}$ and $(\Delta\alpha)_n - (\Delta\alpha)_{n-1}$ are the changes in Δu_o and $\Delta\alpha$ per unit operation from $n-1$ to n, or the rate of change of Δu_o and $\Delta\alpha$, Equation (34) can be written, for the case of very slow rate of change, as

$$\frac{1}{U_\infty}\frac{d(\Delta u_o)}{dn} + i\frac{u_{oo}}{U_\infty}\frac{d(\Delta\alpha)}{dn} = \Psi\frac{\Delta u_o}{U_\infty} + \Phi\frac{u_{oo}}{U_\infty}\Delta\alpha \tag{35}$$

which represents a system of first-order homogeneous differential equations with unknown Δu_o and $\Delta\alpha$. On assuming solutions of the form

$$\frac{\Delta u_o}{U_\infty} = u_o e^{kn} \quad \text{and} \quad \frac{u_{oo}}{U_\infty}(\Delta\alpha) = \lambda_o e^{kn}$$

the following characteristic equation is obtained

$$\begin{vmatrix} \Psi_r - k & \Phi_r \\ \Psi_i & \Phi_i - k \end{vmatrix} = 0 \tag{36}$$

where r and i denote real and imaginary parts, respectively. The growth or decay of Δu_o and $\Delta\alpha$ is discriminated by applying the Hurwitz-Routh criteria. For a stable solution, i.e. decay of the deviations from the neutral state, the conditions

$$\begin{aligned} &(a) \qquad -(\Psi_r + \Phi_i) > 0 \\ &(b) \qquad \Psi_r\varphi_i - \varphi_r\Psi_i > 0 \end{aligned} \tag{37}$$

must be met.

The previously raised question of the stability at the synchronization stage can now be tackled on the assumption that there is a very slow time-wise change of the deviations Δu_o and $\Delta\alpha$. In such case the problem of stability at synchronization is equivalent to the problem of the convergence of the foregoing iterative process. Then Equation (37) may be regarded as the stability criterion for synchronization.

Upon integration, as in Equation (29), Equation (31) yields

$$\frac{u_o}{U_\infty} e^{i\alpha} = i \frac{A}{S'}\left[e^{-iS' \frac{1}{a} f\left(\frac{2u_o}{U_\infty}\right)} + e^{-iS'b}\right] e^{i\alpha} + \frac{u_v}{U_\infty}$$

$$\text{for} \quad b > \frac{1}{a} f\left(\frac{2u_o}{U_\infty}\right) \tag{38}$$

or

$$\frac{u_o}{U_\infty} e^{i\alpha} = i \frac{A}{S'}\left[2e^{-iS' \frac{1}{a} f\left(\frac{2u_o}{U_\infty}\right)}\right] e^{i\alpha} + \frac{u_v}{U_\infty}$$

$$\text{for} \quad b < \frac{1}{a} f\left(\frac{2u_o}{U_\infty}\right)$$

and the corresponding stability criterion, Equation (37), with the use of (38), is

$$(I) \qquad 1 - Eq \cos\left[S' \frac{1}{a} f\left(\frac{2u_{oo}}{U_\infty}\right)\right] + D \cos \alpha_o > 0$$

$$\text{(II)} \qquad D \cos \alpha_o \left\{ 1 - Eq \cos \left[S' \frac{1}{a} f\left(\frac{2u_{oo}}{U_\infty} \right) \right] \right\}$$

$$- D\, Eq \sin \alpha_o \sin \left[S' \frac{1}{a} f\left(\frac{2u_{oo}}{U_\infty} \right) \right] > 0 \tag{39}$$

where

$$q = 1 \quad \text{for} \quad b > \frac{1}{a} f\left(\frac{2u_o}{U_\infty} \right)$$

$$q = 2 \quad \text{for} \quad b < \frac{1}{a} f\left(\frac{2u_o}{U_\infty} \right)$$

$$D = \frac{u_v}{u_{oo}} \quad \text{and} \quad E = \frac{A}{a} \left[\frac{d}{d \frac{u_o}{U_\infty}} f\left(\frac{2u_o}{U_\infty} \right) \right]_{u_o = u_{oo}}$$

SYNCHRONIZATION SIGNAL FROM THE BLADE VIBRATION AND HYDRODYNAMIC REACTION OF THE SHED VORTICES

In order to complete the closed loop shown in Figure 2, the synchronization signal due to the blade vibration and the hydrodynamic reaction of the shed vortices upon the blade should be evaluated. In the mathematical treatments of those two quantities, the blade is assumed to be a flat plate, and the thin-airfoil method is used. The corresponding coordinate system is shown in Figure 8.

SYNCHRONIZATION SIGNAL DUE TO BLADE VIBRATION

The flow in the system under consideration is composed of two parts. One is "no circulation" flow due to the blade vibration and the other is the flow with circulation due to the shed vortices. "No circulation" means that the total circulation around the body is zero. In Equation (31) or (38), that flow velocity at the separation points which is due to the "no circulation" part is u_v, and that due to the total flow is u_o. Derivation of u_v for the assumed mode of blade vibration follows.

Consider the bound-vortex distribution

$$\gamma_b(x,t) = \gamma_{bo}(x)\, e^{i\omega' t}$$

$$= 2U_\infty\left[A_o \frac{\cos\varphi}{\sin\varphi} - \frac{1}{2} A_1 \frac{\cos 2\varphi}{\sin\varphi} + \sum_{n=2}^{\infty} A_n \sin n\varphi\right] e^{i\omega' t} \tag{40}$$

where $x = -\frac{C}{2}(1 + \cos\varphi)$ and C is the chord length. Clearly, this bound-vortex distribution satisfies the "no circulation" condition

$$\int_{-C}^{0} \gamma_{bo}(x)\, dx = 0 \tag{41}$$

The strength of the bound-vortex distribution near the trailing edge

$\varphi = \pi - \epsilon$, where $\pi >> \epsilon > 0$, is given by

$$\gamma_{bo}(\varphi = \pi - \epsilon) \sim -2U_\infty(A_o + \frac{1}{2} A_1) \frac{1}{\epsilon} \tag{42}$$

Therefore, if $\varphi = \pi - \epsilon$ denotes the coordinate of the flow separation points,

$$u_{vu} = -u_{v\ell} = -U_\infty(A_o + \frac{1}{2} A_1) \frac{1}{\epsilon} \tag{43}$$

This satisfies the symmetrical relation Equation (30), and u_v can be written as

$$u_v = -U_\infty(A_o + \frac{1}{2} A_1) \frac{1}{\epsilon} \tag{44}$$

For a particular vibration mode, A_o and A_1 are determined as follows: The induced velocity of the bound vortex in the y-direction is

$$\begin{aligned} v_i(x\cdot t) &= \frac{1}{2\pi}\int_{-C}^{\rho} \frac{\gamma_{bo}(\xi)}{\xi - x}\, d\xi\, e^{i\omega' t} \\ &= U_\infty\left[- A_o + \Sigma A_n \cos n\varphi\right] e^{i\omega' t} \end{aligned} \tag{45}$$

If the vibrational velocity of the blade in the y-direction is given by

$$v_b(x,t) = U_\infty g(x)\, e^{i\omega' t} \tag{46}$$

then the boundary condition on the blade requires that

$$v_i(x,t) - (\frac{\partial}{\partial t} + U \frac{\partial}{\partial x})\, y_b = 0$$

where y_b is the vibrational displacement of the blade. The above boundary condition can be written as

$$v_i(x,t) - \left[v_b(x,t) + U_\infty \frac{\partial}{\partial x} \int_o^t v_b(x,t)\, dt\right] = 0$$

and therefore A_o and A_1 are determined by

$$- A_o + \sum_{n=1}^{\infty} A_n \cos n\varphi = g(x) - i \frac{U_\infty}{\omega'} g'(x) \tag{47}$$

HYDRODYNAMIC REACTION FORCE ON THE BLADE DUE TO THE SHED VORTICES

To ascertain the existence of self-exciting singing, the vibratory force exerted on the blade, due to the bound vortex and to shed vortices, has to be evaluated and its phase compared to the vibration velocity of the blade.

The hydrodynamic force exerted by the "non-circulatory" component of the bound-vortex distribution corresponding to any blade vibrational mode has a virtual-mass term only and no damping component. On the other hand, the reaction force of the shed vortices has a damping, as well as a virtual-mass, component. Therefore, for the discussion on the existence of self-exciting vibration, only the latter hydrodynamic force should be taken into account.

The reaction force due to the shed vortices is evaluated by the method used by Kármán and Sears in non-stationary wing theory.[8] As is shown in Figure 8, the shed vortices are assumed to be flowed away along the x-axis. The shed vortices have their counter vortices on the blades; these are known as bound vortices. Thus the flow system due to the shed vortices is composed of the vortex pairs. Then the momentum in the y-direction due to the i^{th} vortex pair is given by

$$I = \rho\Gamma_i (x_{si} - x_{bi}) \tag{48}$$

where ρ , Γ_i , and x_{bi} denote the density of fluid, the circulation of the shed vortex located at x_{si} , and the location of the counter vortex, respectively. The force upon the blade due to the particular pair is

$$F = - \frac{dI}{dt} = -\rho \frac{d}{dt} \Gamma_i (x_{si} - x_{bi}) \tag{49}$$

Assuming for simplicity that the counter vortex is concentrated at the trailing edge (x = 0), Equation (49) becomes

$$F = -\rho \frac{d}{dt} \Gamma_i x_{si} \tag{50}$$

In the present problem, the sum of the vorticity distributions from the upper and the lower separation points yields

$$\Gamma_i = 2e^{i\alpha} U_\infty H \left[\frac{1}{a} f\left(\frac{2u_o}{U_\infty}\right)\right] e^{i[\omega' t - S' x]} \, dx \tag{51}$$

where the time origin is the same as in the case of Equation (31). The total force acting upon the blade is then given by

$$F_b = -\rho \frac{d}{dt} \int_0^\infty \Gamma_i x dx = \frac{2\rho U_\infty \omega'}{S'} \sqrt{\left(\frac{1}{S'}\right)^2 + w^2} \; e^{i(\alpha + \beta - \tan\beta + \frac{\pi}{2})} \tag{52}$$

where

$$w = \frac{1}{a} f\left(\frac{2u_o}{U_\infty}\right) \quad , \quad \beta = \tan^{-1} wS'$$

If the effective thickness of the blade at the separation point is taken as d ,

$$S' = \frac{\omega' d}{U_\infty}$$

and hence

$$F_b = \frac{1}{2} \rho U_\infty^2 \, d \sqrt{\left(\frac{1}{S'}\right)^2 + w^2} \; e^{i(\alpha + \beta - \tan\beta + \frac{\pi}{2})} \tag{53}$$

EXISTENCE OF THE SELF-EXCITED SINGING STATE

The various constituent elements of the closed loop comprising the propeller-blade vibration and the Kármán vortices-shedding mechanisms having been determined, it is now possible to present a mathematical expression for the existence of the self-excited singing state. In doing so, however, it seems useful to summarize the previously obtained results.

(1) Blade Vibration to Synchronizational Signal

When the vibrational velocity of a point on the blade is given by

$$v_b(x \cdot t) = U_\infty g(x)\, e^{i\omega' t} \tag{46}$$

the synchronization signal is expressed in the form of

$$u_v\, e^{i\omega' t} = -\, U_\infty \left(A_o + \frac{1}{2} A_1\right) \frac{1}{\epsilon}\, e^{i\omega' t} \tag{44}$$

where

$$-\, A_o + \sum_{n=1}^{\infty} A_n \cos n\varphi = g(x) - i\, \frac{U_\infty}{\omega'}\, g'(x)\ , \quad x = -\frac{c}{2}\,(1 + \cos\varphi) \tag{47}$$

and $\varphi = \pi - \epsilon\ (\pi >> \epsilon > 0)$ is the location of the separation points.

(2) Synchronized Operation of the Shedding Mechanism with $u_v e^{i\omega' t}$

The governing equation for the synchronization, after use is made of the simplified expression Equation (11), is given by

$$\frac{u_o}{U_\infty}\, e^{i\alpha} = i\, \frac{A}{S'} \left[e^{-S' \frac{1}{a} f\left(\frac{2u_o}{U_\infty}\right)} + e^{iS'b} \right] e^{i\alpha} + \frac{u_v}{U_\infty}$$

$$\text{for} \quad b > \frac{1}{a}\, f\left(\frac{2u_o}{U_\infty}\right)$$

or

$$\frac{u_o}{U_\infty} e^{i\alpha} = i \frac{A}{S'} \left[2e^{-S' \frac{1}{a} f\left(\frac{2u_o}{U_\infty}\right)} \right] e^{i\alpha} + \frac{u_v}{U_\infty}$$

$$\text{for} \quad b < \frac{1}{a} f\left(\frac{2u_o}{U_\infty}\right) \tag{38}$$

Furthermore, the stability of the synchronization state requires that

$$\text{(I)} \qquad 1 - Eq \cos\left[S' \frac{1}{a} f\left(\frac{2u_{oo}}{U_\infty}\right)\right] + D \cos \alpha_o > 0$$

and

$$\text{(II)} \qquad D \cos \alpha_o \left\{1 - Eq \cos\left[S' \frac{1}{a} f\left(\frac{2u_{oo}}{U_\infty}\right)\right]\right\}$$

$$- D\, Eq \sin \alpha_o \sin\left[S' \frac{1}{a} f\left(\frac{2u_{oo}}{U_\infty}\right)\right] > 0 \tag{39}$$

Equations (38) and (39) give u_o and α in the stable synchronized condition for given synchronization signals u_v and S'.

(3) Hydrodynamic Force Reaction Due to the Shed Vortices

When u_o and α are given, the reaction force on the blade is

$$F_b = \frac{1}{2} \rho U_\infty^2 d \sqrt{\left(\frac{1}{S'}\right)^2 + w^2}\; e^{i(\alpha + \beta - \tan \beta + \frac{\pi}{2})} \tag{53}$$

where the origin of time is taken so that u_v has a real positive value.

If the above results are used, the criterion for the positive work of the reaction force upon the blade vibration can be obtained; this is composed of the criteria for the existence of the self-excited singing state together with that of stable synchronization, Equation (39), I or II. In the first place, it may be assumed that the reaction force is concentrated near the trailing edge of the blade. As was stated earlier (p. 23) the "no circulation" component of the bound vortices which is caused by the blade vibration exerts no damping effect. Therefore, if the absolute value of the phase difference between the reaction force $F_b e^{i\omega' t}$ and the vibration velocity of the trailing edge $v_b(o,t) = U_\infty g(o) e^{i\omega' t}$ is less than $\frac{\pi}{2}$, the reaction force should exert positive work upon the blade vibration. As Equation (53) has its phase origin at u_v, the criterion for positive work is given by

$$- \pi < \alpha + \beta - \tan \beta + \theta < 0 \tag{54}$$

where, from Equations (46) and (44),

$$\theta = \arg \frac{u_v e^{i\omega' t}}{v_b(\varphi = \pi - \epsilon, t)} = \arg \frac{-i(A_o + \frac{1}{2} A_1)\frac{1}{\epsilon}}{g(\varphi = \pi - \epsilon)}$$

NUMERICAL CALCULATIONS AND DISCUSSION

FREE SHEDDING OF KÁRMÁN VORTICES

For several values of A, b, and a, the unknown Strouhal number and dimensionless velocity ratio u_o/U_∞ are determined by Equation (29) for the case of free shedding of Kármán vortices. Both these unknowns are determined by solving the real and imaginary parts of the above equation simultaneously. Due to the complicated form of the function $f(2u_o/U_\infty)$ the equations are solved graphically and the corresponding results are summarized in the following table.

	a	A	S_t	u_o/U_∞
b = 2	2	$1/2\pi$	0.202	0.141
	2	$0.8/2\pi$	0.197	0.127
	1	$0.6/2\pi$	0.175	0.145
	2	$0.6/2\pi$	0.191	0.110
	3	$0.6/2\pi$	0.200	0.080
	2	$0.5/2\pi$	0.185	0.099

The parameters A and b, which are shape parameters, can be selected according to the particular body shape. The parameter a, however, which is related to the rate of growth of the disturbance in the vortex sheet, can only be selected by trial. The selected values of A and b seem to be reasonable ones, since ($A = \frac{1}{2\pi}$, $b = 2$) and ($A = \frac{0.6}{2\pi}$, $b = 2$) describe approximately the circular cylinder body and parabolic trailing-edge body. The corresponding value of Strouhal number (around 0.2) seems very close to the usual experimental results. The values of u_o/U_∞ seem reasonable also. This is an indication that, in spite of all the assumptions made, the present mathematical model for the free-shedding mechanism is promising.

SELF-EXCITED SINGING

A series of numerical calculations was made to illustrate the existence of the self-excited singing and to clarify its mechanism. As is seen in Figure 9a, the following vibrational modes of the blade have been considered:

(a) 1st mode: spanwise bending mode, with $g(x) = h =$ constant

(b) 2nd mode: torsional mode, with $g(x) = - h \cos \varphi$

(c) 3rd mode: chordwise bending mode, with $g(x) = h \cos 2\varphi$

where the transformation from Cartesian to angular coordinates is given by $x = - \frac{C}{2}(1+\cos \varphi)$, C = chord length of blade. The ratio of the separation-point thickness d to the chord length C is 0.1 .

The numerical work has been performed along the line indicated in the section on existence of the self-excited singing state (p. 25). In the first place, the real and imaginary parts of Equation (38) are solved simultaneously with respect to u_o/U_∞ and α for given u_v/U_∞ and S'. It may be useful, here, to note the following points:

(1) u_v/U_∞ , the trigger signal for the synchronization of the vortex shedding with the blade vibration, is proportional to the amplitude of the blade vibration and is nothing but the amplitude of the blade vibration expressed in hydrodynamical terms.

(2) $S' = \omega' d/U_\infty$ is the non-dimensional expression of the natural frequency of the blade vibration ω' (= the strong singing frequency) in terms of the blade thickness at the separation points, d , and the flow velocity at infinity, U_∞ . The expression S'/S will be used in place of S', where $S = \omega d/U_\infty$, and ω is the free-shedding angular frequency of the vortices. Since $S'/S = \omega'/\omega$, S'/S should be named "tuning factor." Meanwhile, since $S = 2\pi S_t$ (see Equation [28]; S_t is

the Strouhal number) is constant for a given blade shape independent of the flow velocity, and since, furthermore, ω' and d are also constant for the given blade, $S'/S = (\omega' d/2\pi S_t)(1/U_\infty)$ has the sense of a non-dimensional expression of the reciprocal of the flow velocity U_∞.

If the obtained values of u_o/U_∞ and α are applied to Equations (39)-I and (39)-II, the limits are determined for the stability of the synchronization of the vortex shedding with the blade vibration, under the given blade-vibration amplitude u_v/U_∞ and the given tuning factor S'/S. In a similar way, Equation (54) can be used to check and determine whether or not the hydrodynamic reaction of the shed vortices exerts positive work upon the blade vibration.

In the actual calculation, owing to the complicated functional form of $f\left(\frac{2u_o}{U_\infty}\right)$, it is difficult to solve Equation (38) with respect to u_o/U_∞ and α for given u_v/U_∞ and S'/S, and, therefore, an auxiliary procedure is introduced: Equation (38) is solved with respect to u_v/U_∞ and α for assumed u_o/U_∞ and S'/S. This procedure gives, for each value of S'/S, the auxiliary diagrams illustrated in Figures 9b and 9c, on which are also indicated the ranges where the criteria of Equations (39) and (54) are satisfied. From these auxiliary diagrams, the final charts shown in Figures 10a, b, and c are derived. Figures 10a, b, and c exhibit the two kinds of limit boundaries corresponding to the stable-synchronization criterion, Equation (39)-II, and the positive-work criterion, Equation (54), on a u_v/U_∞ versus S'/S plane. Since the condition imposed by Equation (39)-II is always more severe than that imposed by Equation (39)-I, the limit boundary due to the latter is omitted.

The values used in this calculation for the parameters are $A = \frac{0.6}{2\pi}$, $b = 2$, and $a = 1, 2, 3$. The first two are approximating values for a parabolic shape of the trailing edge of the body. On the other hand, the given values of a are mere trial. However, although the choice of a causes some quantitative effect, as seen in Figures 10a, b, and c, the qualitative nature does not seem to be altered.

It should be noted that Figures 10a, b, and c indicate whether or not the assumed value of u_v/U_∞ satisfies the two criteria, but give no information with regard to the determination of u_v/U_∞ . This is the problem of the limit-cycle amplitude of the blade vibration, which should be resolved by considering the balance between the energy input due to the hydrodynamic reaction force from the shed vortices, $F_b e^{i\omega' t}$, and the energy dissipation due to the damping capacity of the blade. In regard to this point, it should be repeated that the non-circulation flow component due to the blade vibration exerts no damping effect, and, therefore, only the mechanical damping should be considered as the damping capacity of the blade. The existence of the limit cycle should be proved through a strict mathematical consideration, but it may be anticipated by the fact that the magnitude of the reaction force F_b is not affected by the amplitude of the blade vibration as much as the mechanical damping force is affected. With increasing amplitude of blade vibration, the reaction force remains almost unchanged, whereas the damping force increases so that an energy balance due to these forces will eventually appear. If the mechanical damping of the blade is known, one may obtain the locus of the limit-cycle amplitude on a u_v/U_∞ versus S'/S plane (that is, an amplitude versus reciprocal-of-the-flow-velocity plane). If the locus exists in the region bounded by the two kinds of criterion limits (the region indicated by mark $\longleftrightarrow$ in Figures 10a, b, and c) through a certain range of S'/S , then the self-excited strong singing which manifests itself as a step on the frequency-versus-velocity diagram may appear through the corresponding range of the flow velocity. When the limit-cycle locus cuts the stable-synchronization limit, the synchronization of shed vortices with blade vibration may cease. In other words, the closed loop shown in Figure 2 is opened, and consequently there should be a jump from the self-excited strong singing state to the weak one with the Strouhal frequency. While, as seen in Figures 10a, b, and c, the stable synchronization limit seems to occur always as a lower boundary below which the stability is lost, the positive-work limit manifests itself either as an upper or a lower boundary, above or below which, respectively, the favorable phase relation between the blade vibration and the hydrodynamic reaction $F_b e^{i\omega' t}$ vanishes. When this limit makes an upper boundary, the limit-cycle locus does not go up across the limit, because above this boundary the positive work done by the reaction force can no longer be expected, and further increase in the limit-cycle amplitude is impossible. On the other hand, when the positive work limit appears as a lower boundary, the locus can cross the limit, and once the crossing occurs the amplitude of the blade vibration suddenly drops to a low value at which the synchronized shedding condition is lost. In this case, even if the positive work limit exists above the stable-synchronization limit, the jump from the strong singing state to the weak one should appear at this crossing.

Thus the particular feature in the singing-frequency-versus-flow-velocity relation is interpreted by the self-exciting model. Further, provided that the mode shape of blade vibration and its mechanical damping are given, the quantitative derivation of the frequency-versus-velocity diagram is also possible, at least in principle. Before entering into these quantitative details, however, the assumptions and simplifications adopted in the mathematical development should be refined and reinforced. Investigation of most of them is left for future work, but some discussion is offered below.

The approximations given for the mathematical expressions of the influence functions $S_1(x)$ and $S_2(x)$ do not seem to alter the nature of the problem, at least qualitatively. Their essential function as factors determining the vortex-shedding frequency comes from the fact that $S_1(x)$ has a finite value starting with $x = 0$, while $S_2(x)$ is zero at $x = 0$ and has a finite incubation interval before the rapid increase with x and later diminishing; and these characteristics of $S_1(x)$ and $S_2(x)$ are kept in the simplified expressions of Equation (11).

Another speculative assumption was made concerning the concentrating process of the vorticity. To treat the vortex-shedding process in this way instead of solving the Navier-Stokes equation may be allowable when the Reynolds number is not so low and the transportation of the vorticity by flow is dominant compared with the diffusion of the vorticity due to viscosity. For such a case, the most reliable method is to trace the path of each vortex element shed from the separation points, in the manner utilized by Rosenhead for the Helmholtz instability problem. This seems within the capacity of the ordinary computer. In the present work, however, this numerical process was replaced by a largely simplified mathematical model, in order to introduce into the hydrodynamic problem — as generally as possible — the concepts developed in the non-linear oscillation theory, and to clarify the present version of the singing phenomenon as self-excited.

CONCLUSIONS

A model for the propeller-singing phenomenon considered as a self-excited oscillation was presented to interpret the step and jump characteristics in the singing-frequency-versus-flow-velocity diagram.

The singing system was simulated by a "closed loop" composed of a blade as a mechanical vibration system anJ the vortices-shedding mechanism which is responsible for the shedding of vortices in synchronization with blade vibration. The numerical calculations made for several types of blade-vibration mode shape showed that the criteria for the stability of the synchronized shedding of vortices, together with the criterion for the phase relation favorable to positive work done by the hydrodynamic reaction force of the shed vortices upon the blade vibration, can interpret the step and jump phenomenon.

In order to introduce the concepts of the non-linear oscillation theory into the hydrodynamic problem as generally as possible, large simplifications were made in the mathematical expressions, and consequently the quantitative detailed treatment required for each particular case is left for future work.

REFERENCES

1. KRIVSTOV, Y. V. and PERNIK, A. J., "The Singing of Propellers," DTMB Translation 281, October 1958.

2. FUNG, Y. C., An Introduction to the Theory of Aeroelasticity. John Wiley & Sons, New York, 1955, p. 73 (this page contains reference to experiments performed by Kármán and Dunn).

3. ARNOLD, L., LANE, F., and SLUTSKY, S., "Propeller Singing Analysis," General Applied Science Laboratory, Technical Report No. 221.

4. MINORSKY, N., Nonlinear Oscillations. D. Van Nostrand Co., Princeton, N. J., 1962, p. 438.

5. HELMHOLTZ, H., "Uber Discontinuierliche Flussigkeitsbewegungen," Monatsbericht, Berlin. Akad. (1868), p. 215. Reprinted in Phil. Mag. 36, 337 (1868).

6. ROSENHEAD, L., "The Formation of Vortices from a Surface of Discontinuity," Proc. Roy. Soc. A.134, 170 (1932).

7. MINORSKY, N., op. cit., p. 439.

8. KÁRMÁN, T. von, and SEARS, W. R., "Airfoil Theory for Non-Uniform Motion," J. Aeron. Sci. 5, 379 (1937-38).

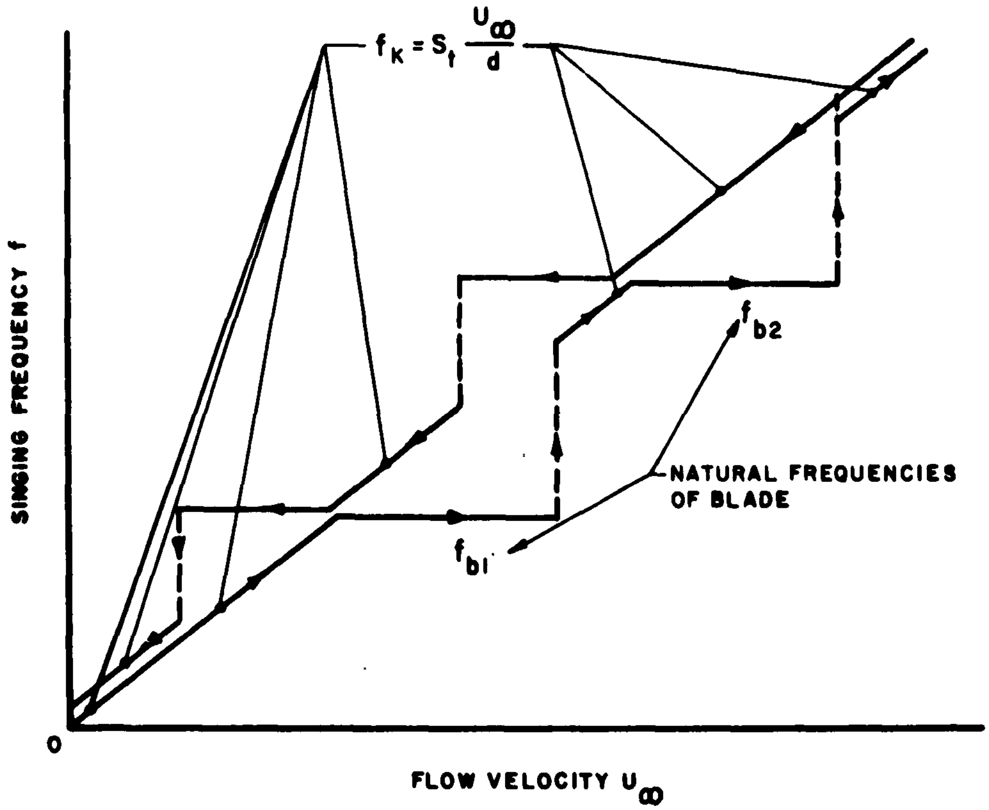

FIGURE I. THE RELATION OF SINGING FREQUENCY VERSUS FLOW VELOCITY

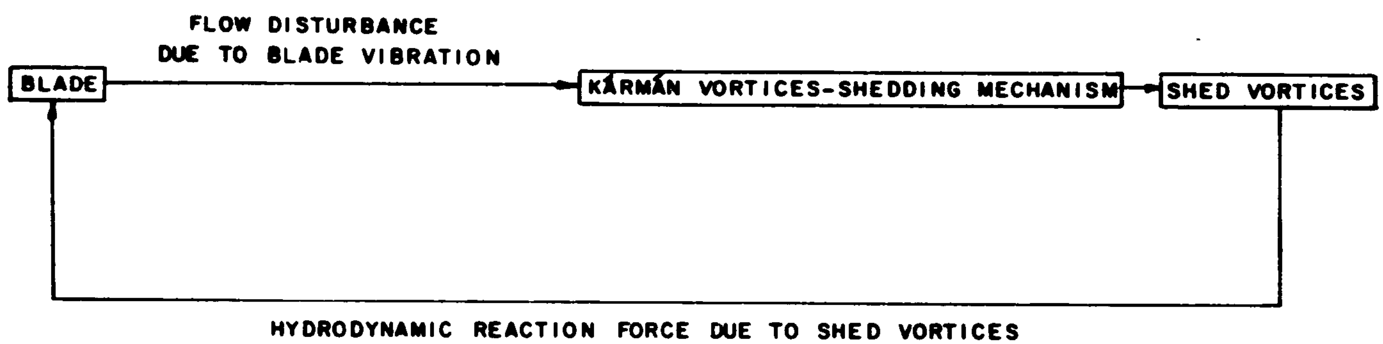

FIGURE 2. CLOSED LOOP FOR THE SELF-EXCITED SINGING

R-1059

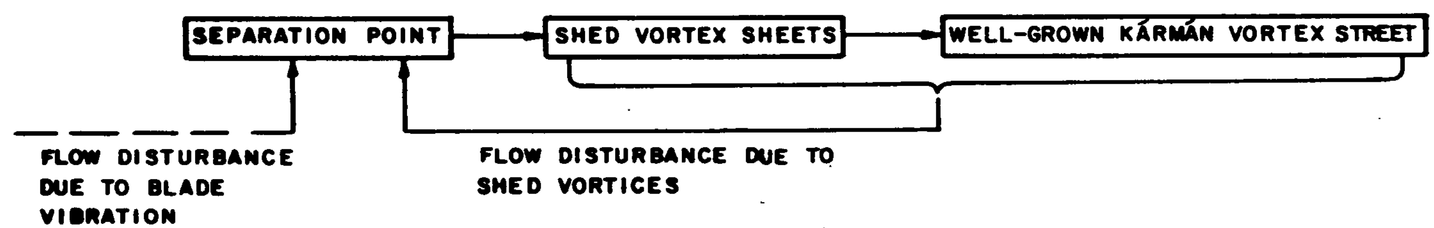

FIGURE 3a. CLOSED LOOP FOR THE VORTEX-SHEDDING MECHANISM

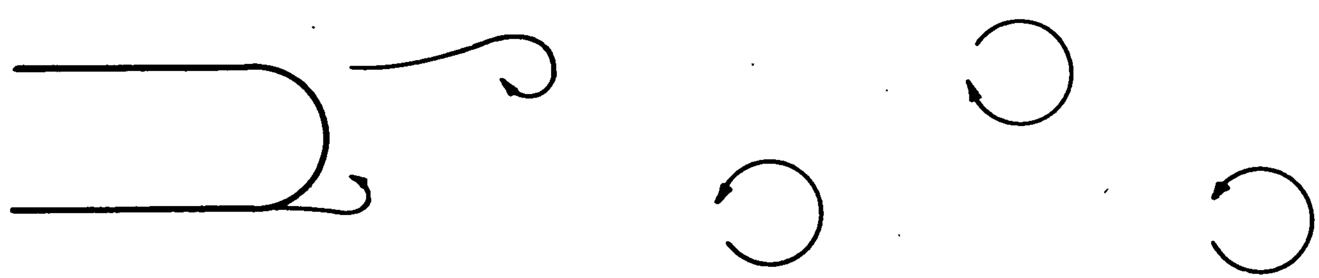

FIGURE 3b. SCHEMATIC FIGURE FOR THE VORTEX-SHEDDING PROCESS

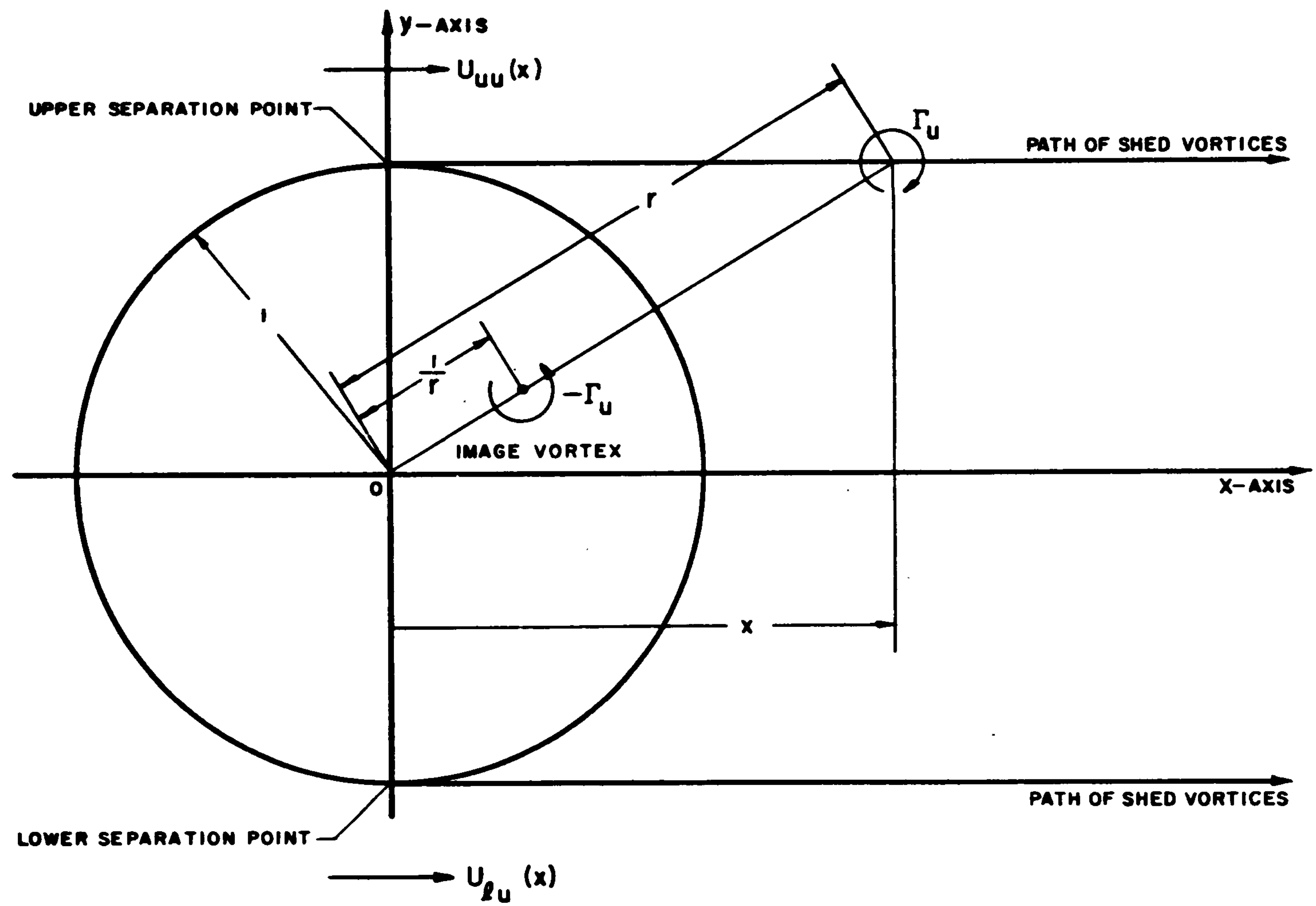

FIGURE 4a. CIRCULAR CYLINDER AND ITS COORDINATE SYSTEM

R-1059

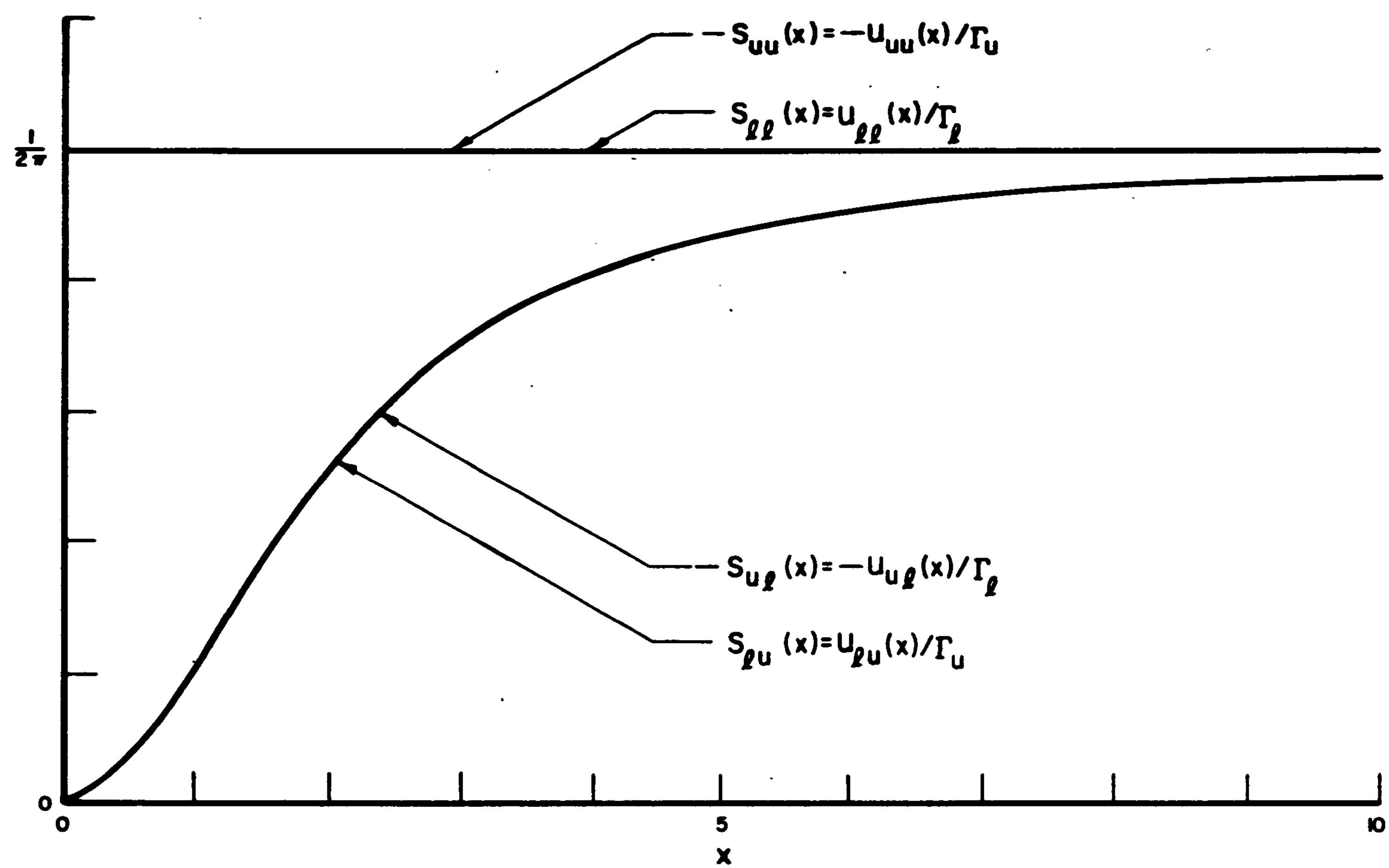

FIGURE 4b. INFLUENCE FUNCTIONS: $S_{uu}(x)$, $S_{u\ell}(x)$, $S_{\ell\ell}(x)$ AND $S_{\ell u}(x)$ FOR CIRCULAR CYLINDER

R-1059

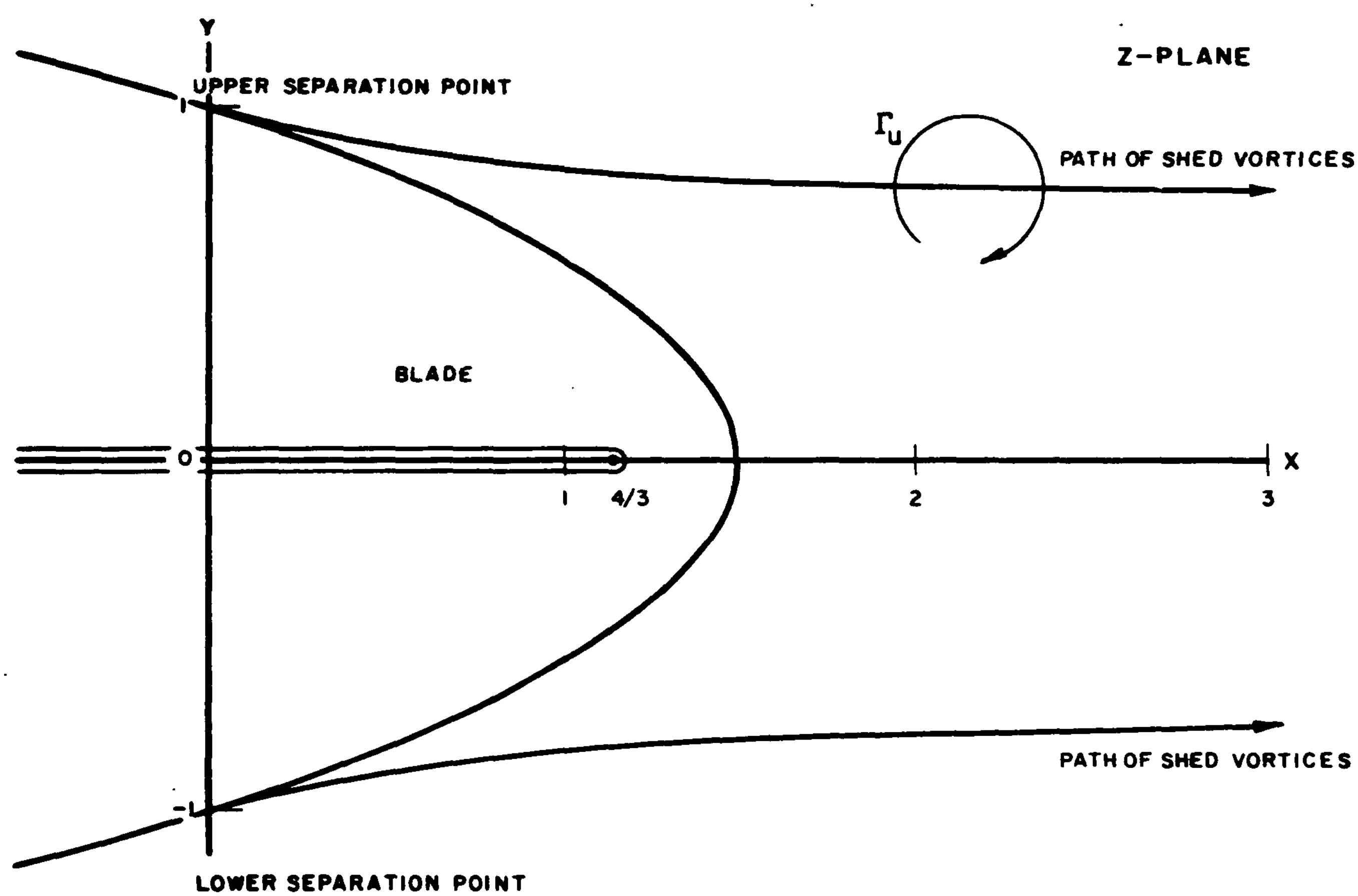

FIGURE 5a. PARABOLA – SHAPED TRAILING-EDGE BLADE AND ITS COORDINATE SYSTEM

R-1059

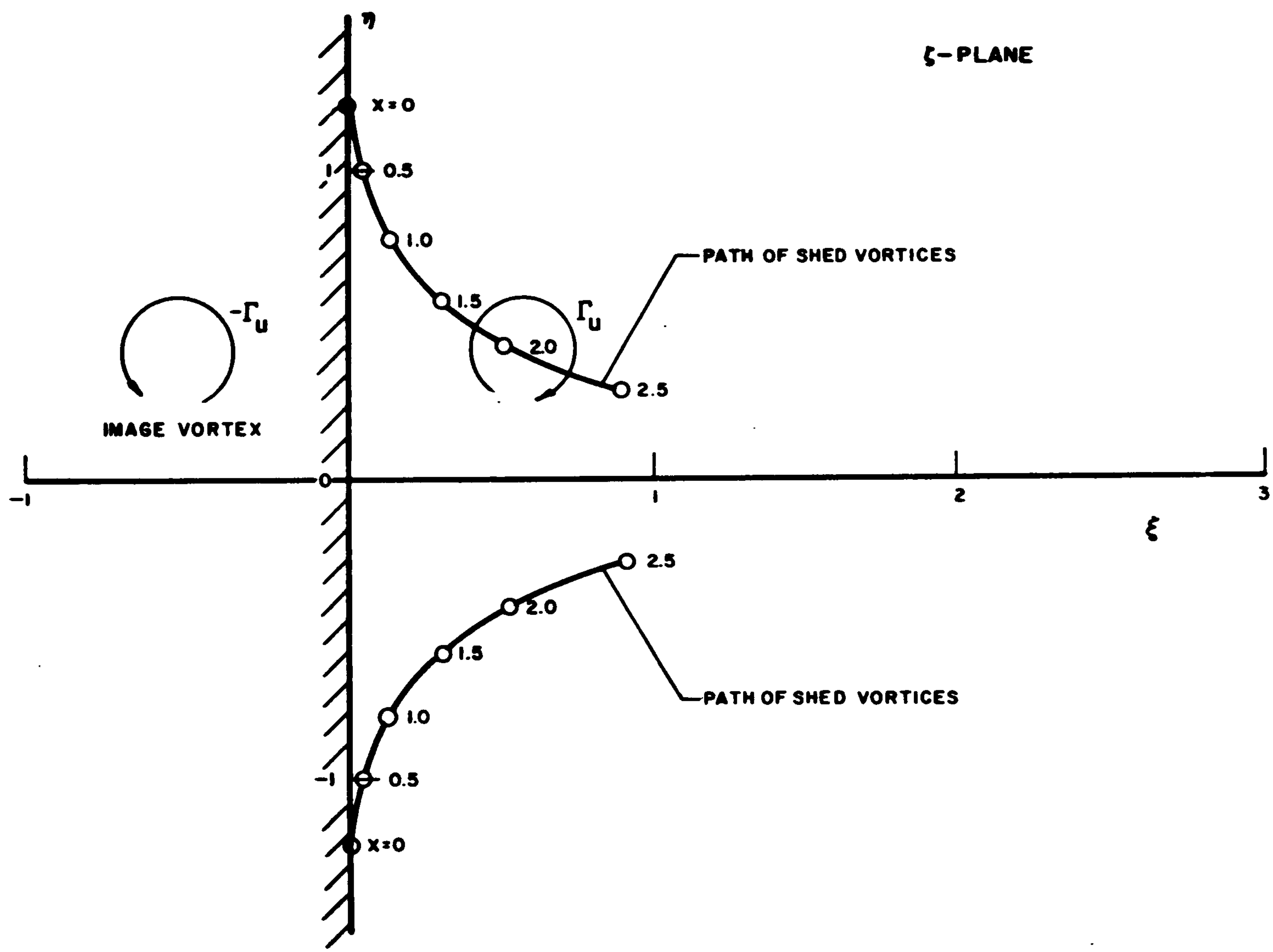

FIGURE 5b. TRANSFORMED PLANE

R-1059

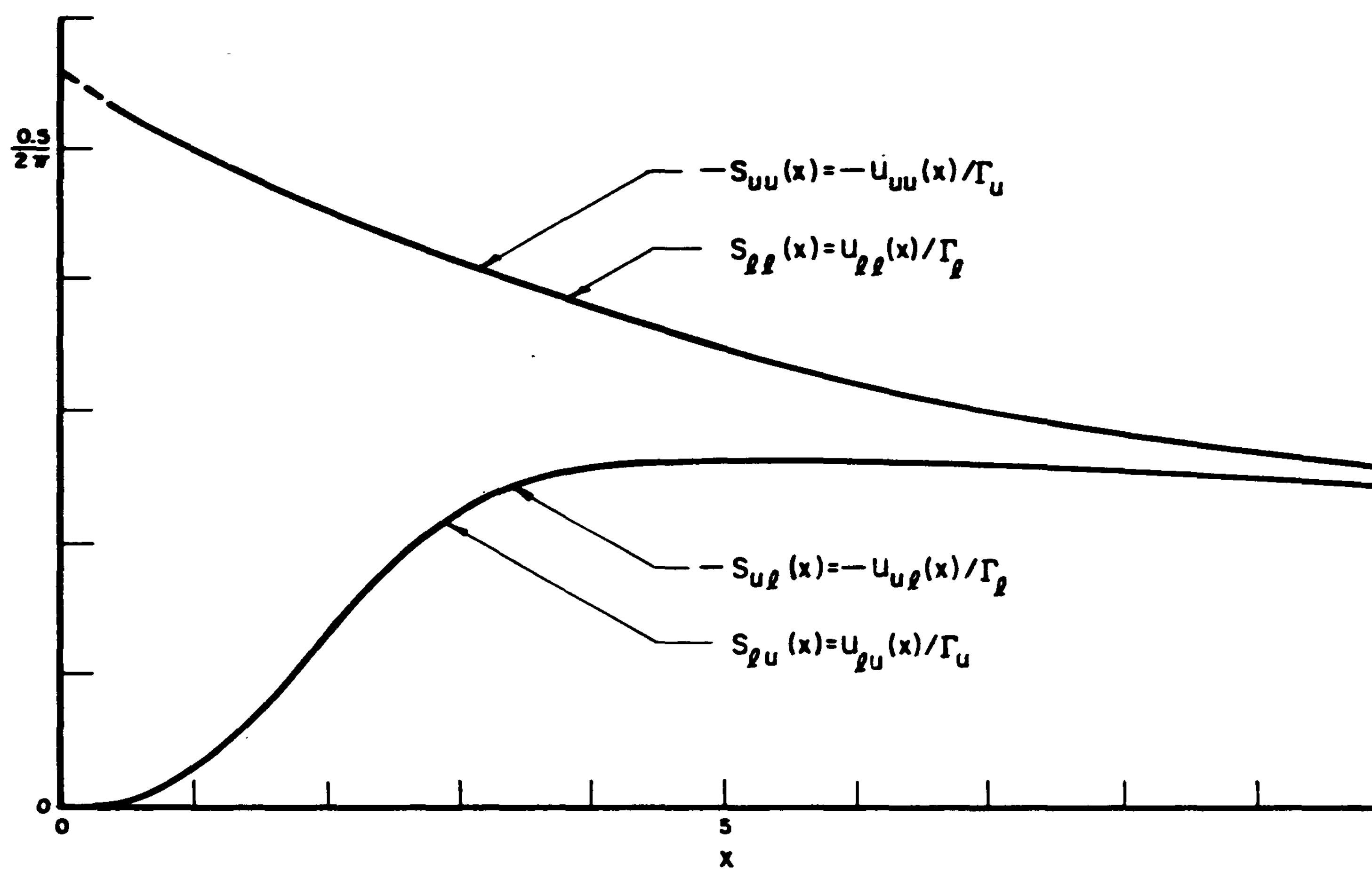

FIGURE 5c. INFLUENCE FUNCTIONS: $S_{uu}(x)$, $S_{u\ell}(x)$, $S_{\ell\ell}(x)$ AND $S_{\ell u}(x)$ FOR PARABOLA-SHAPED TRAILING-EDGE BLADE

R-1059

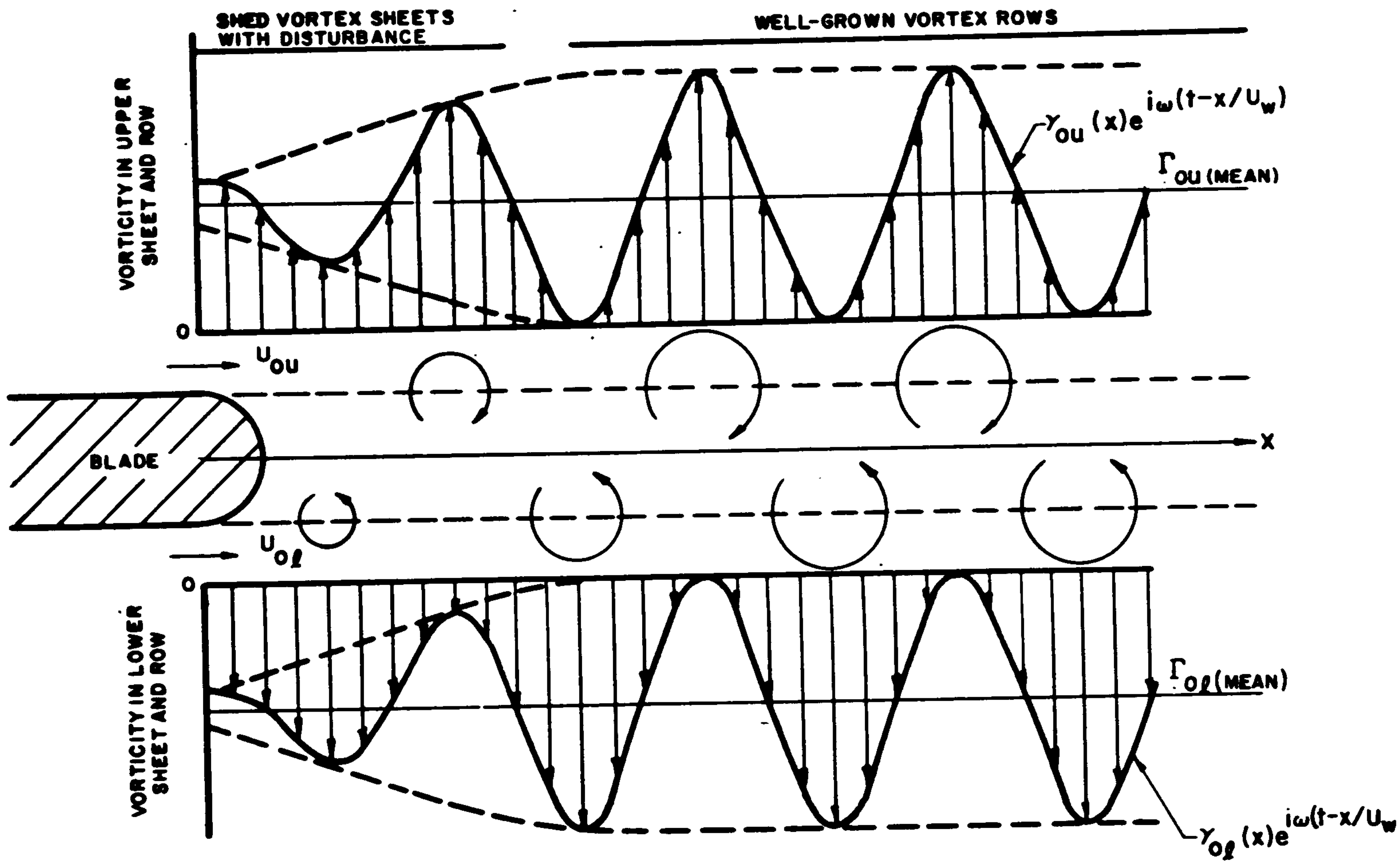

FIGURE 6. CONCENTRATION PROCESS, THE VORTEX SHEET INTO DISCRETE VORTEX ROWS

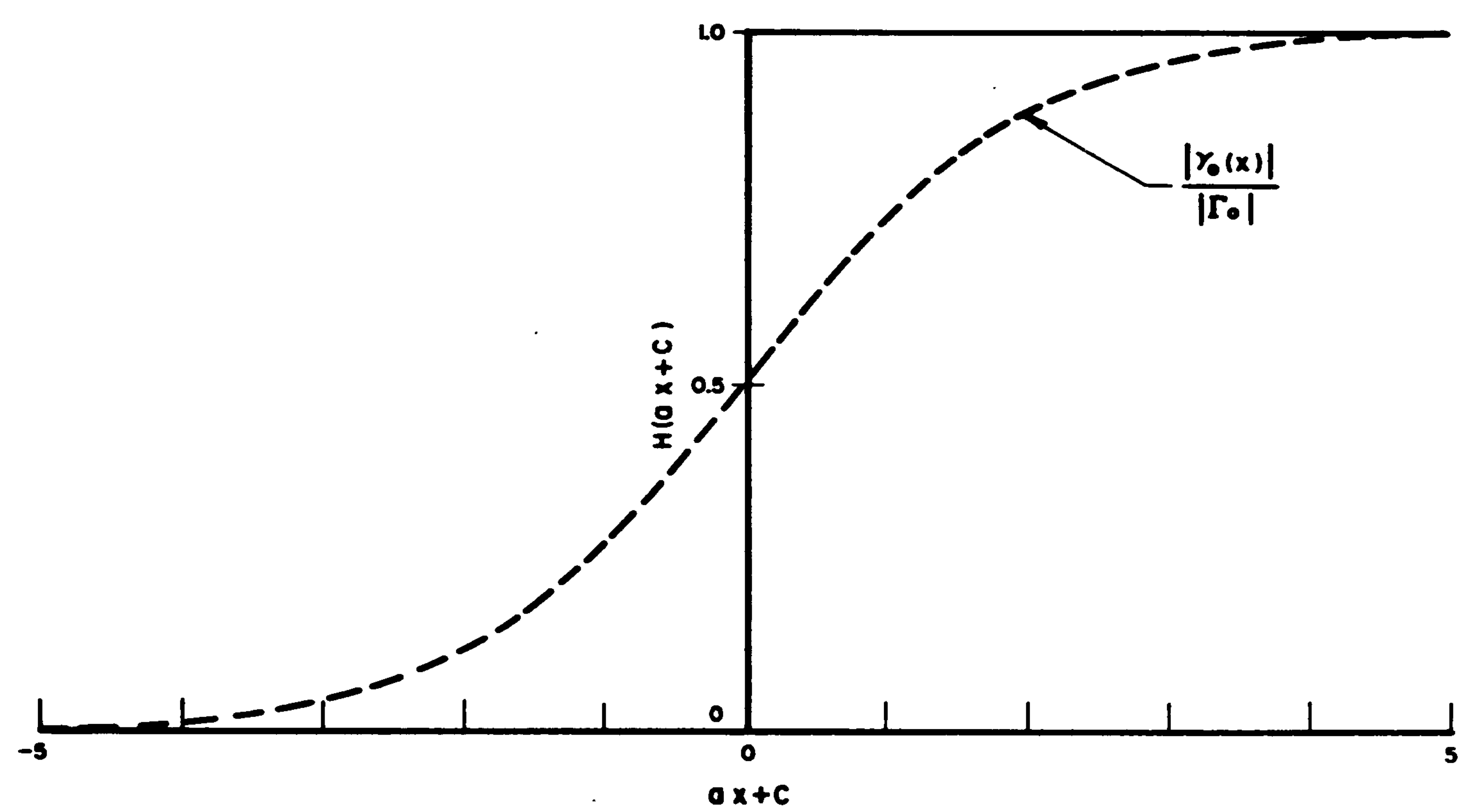

FIGURE 7. APPROXIMATION FOR GROWTH PROCESS OF VORTICITY DISTURBANCE

R-1059

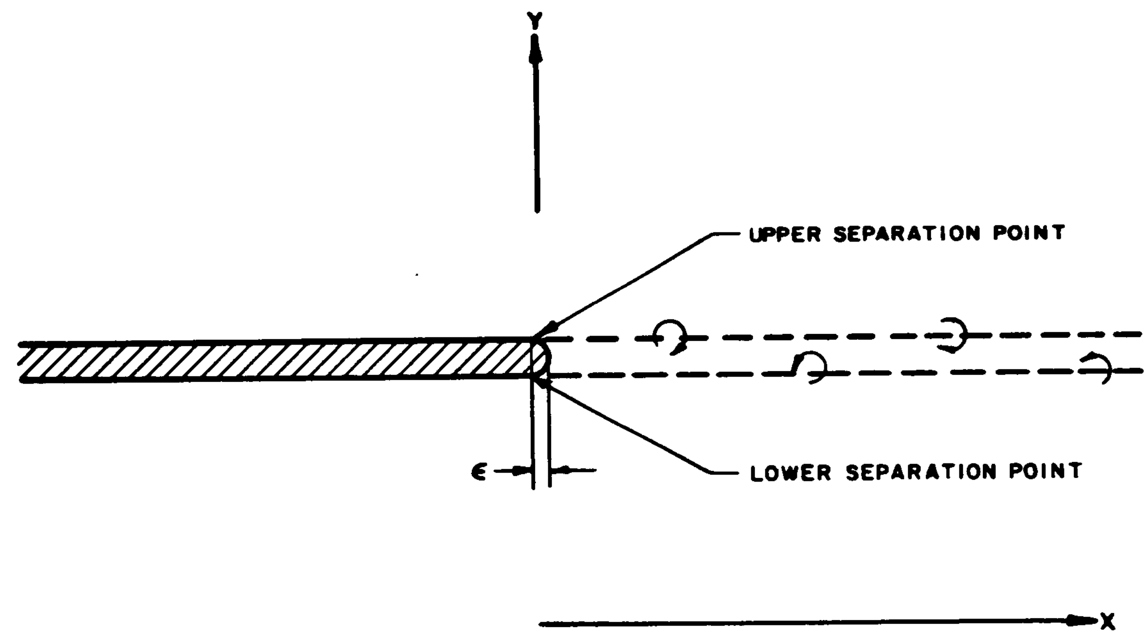

FIGURE 8. COORDINATE SYSTEM FOR FLAT-PLATE BLADE

R-1059

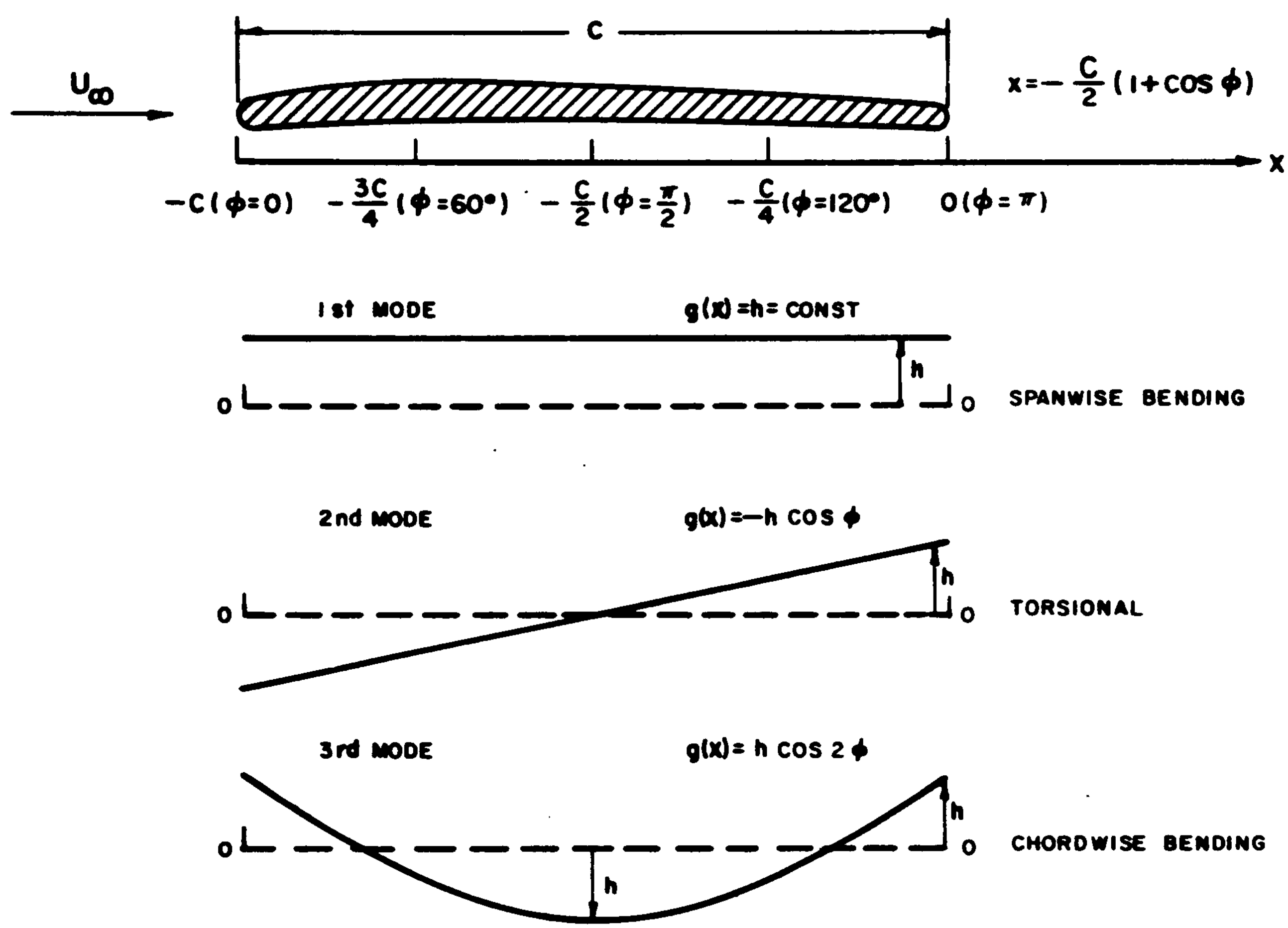

FIGURE 9a. ASSUMED VIBRATION MODE OF BLADE

R-1059

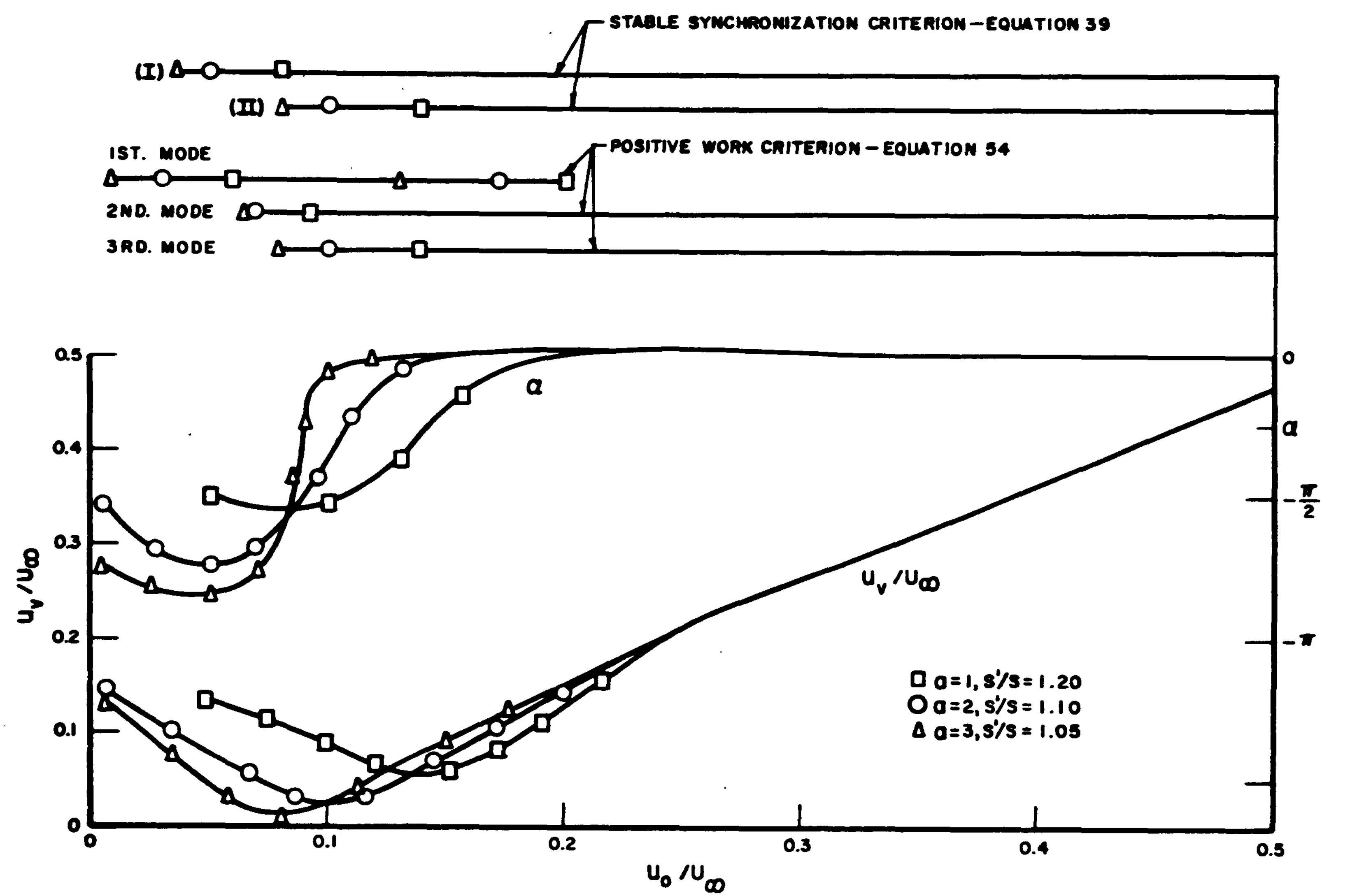

FIGURE 9b. EXAMPLE OF AUXILIARY DIAGRAM FOR $A=0.6/2\pi$, $b=2$, $S'=1.32$ AND $a=1,2,3$ CORRESPONDING TO $S'/S=1.20$, 1.10 AND 1.05 RESPECTIVELY

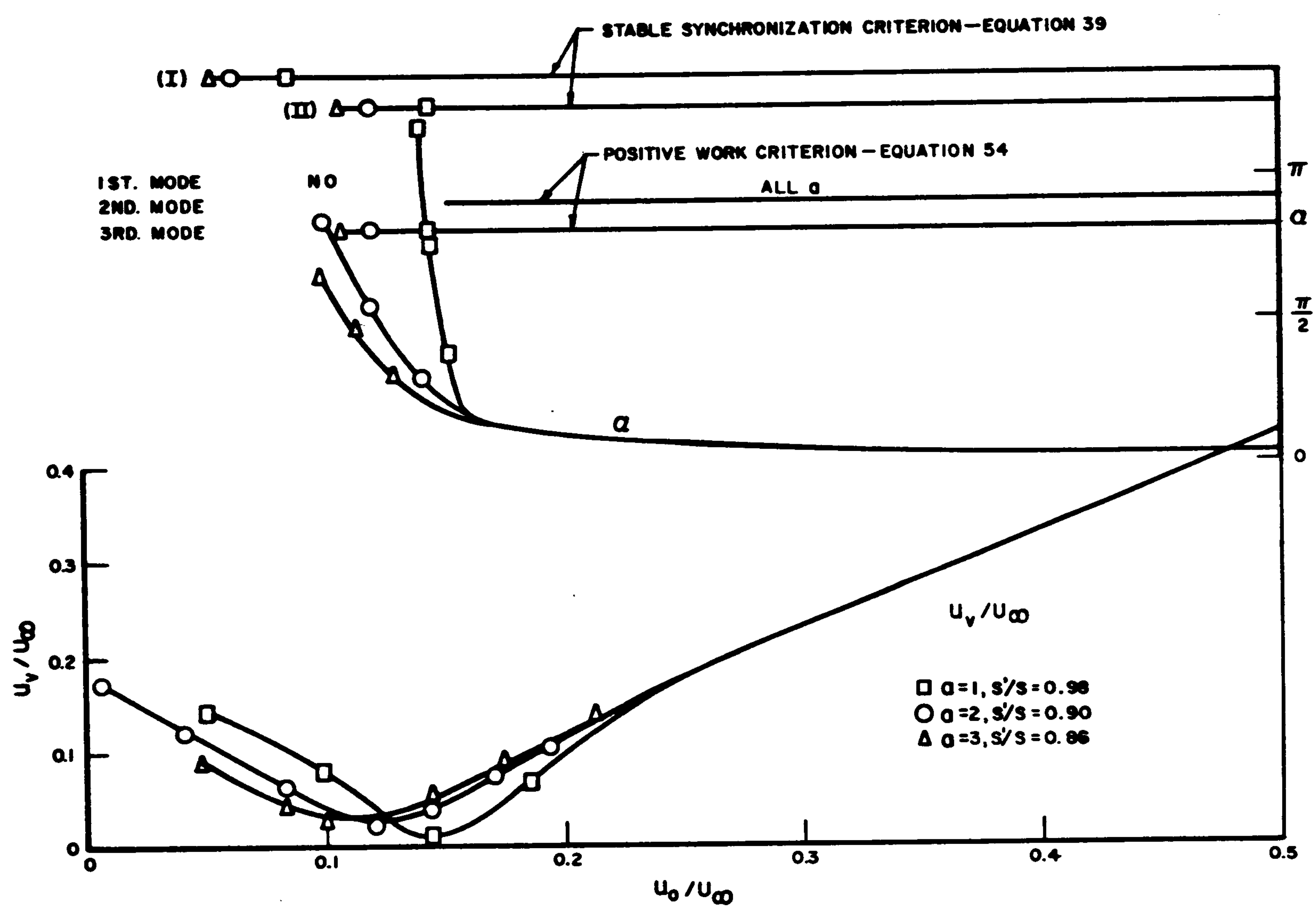

FIGURE 9c. EXAMPLE OF AUXILIARY DIAGRAM FOR $A=0.6/2\pi$, $b=2$, $S'=1.08$ AND $a=1,2,3$ CORRESPONDING TO $S'/S=0.98$, 0.90 AND 0.86 RESPECTIVELY

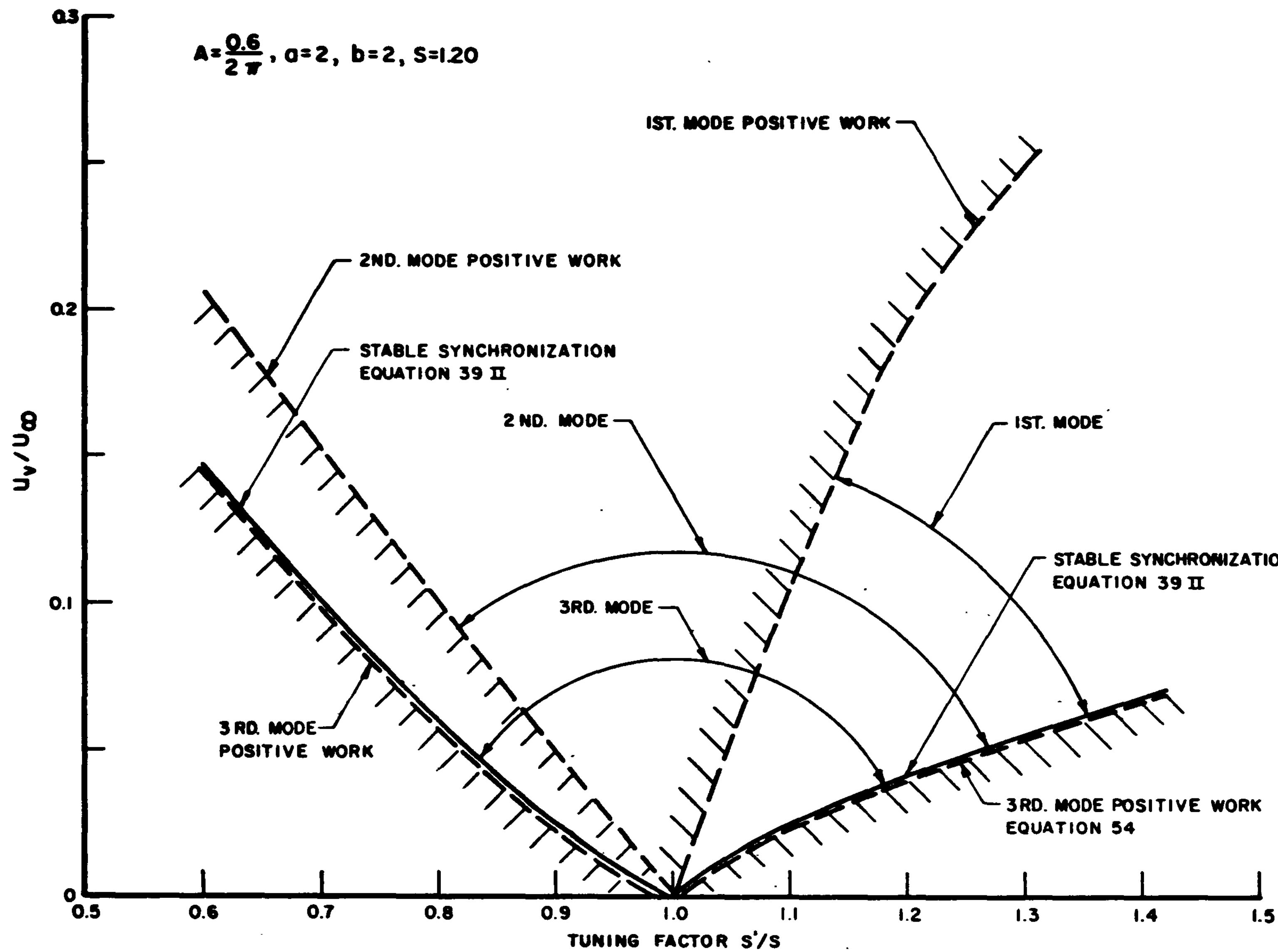

FIGURE 10a. EXISTENCE REGION OF SELF-EXCITED SINGING

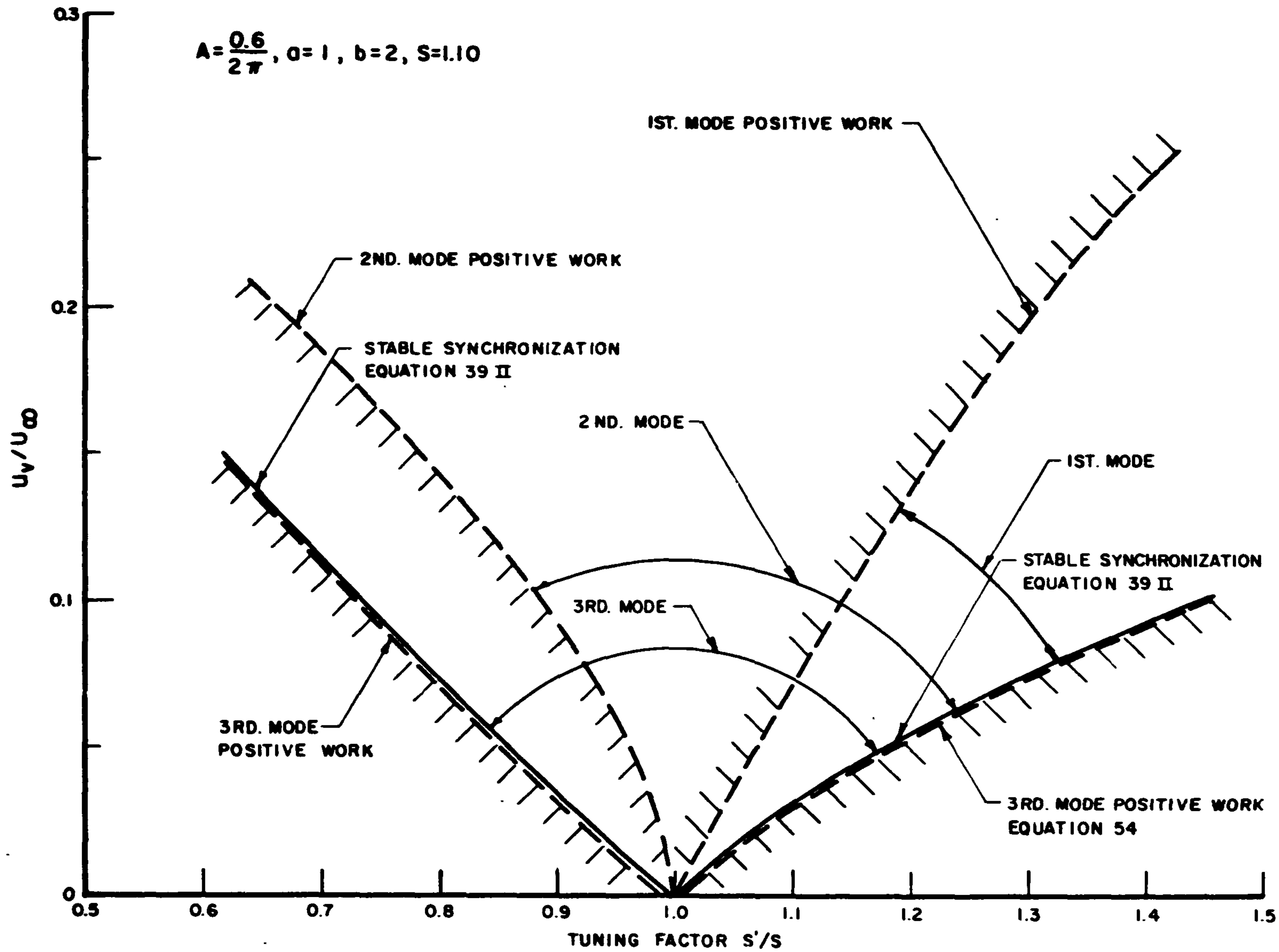

FIGURE 10b. EXISTENCE REGION OF SELF-EXCITED SINGING

R-1059

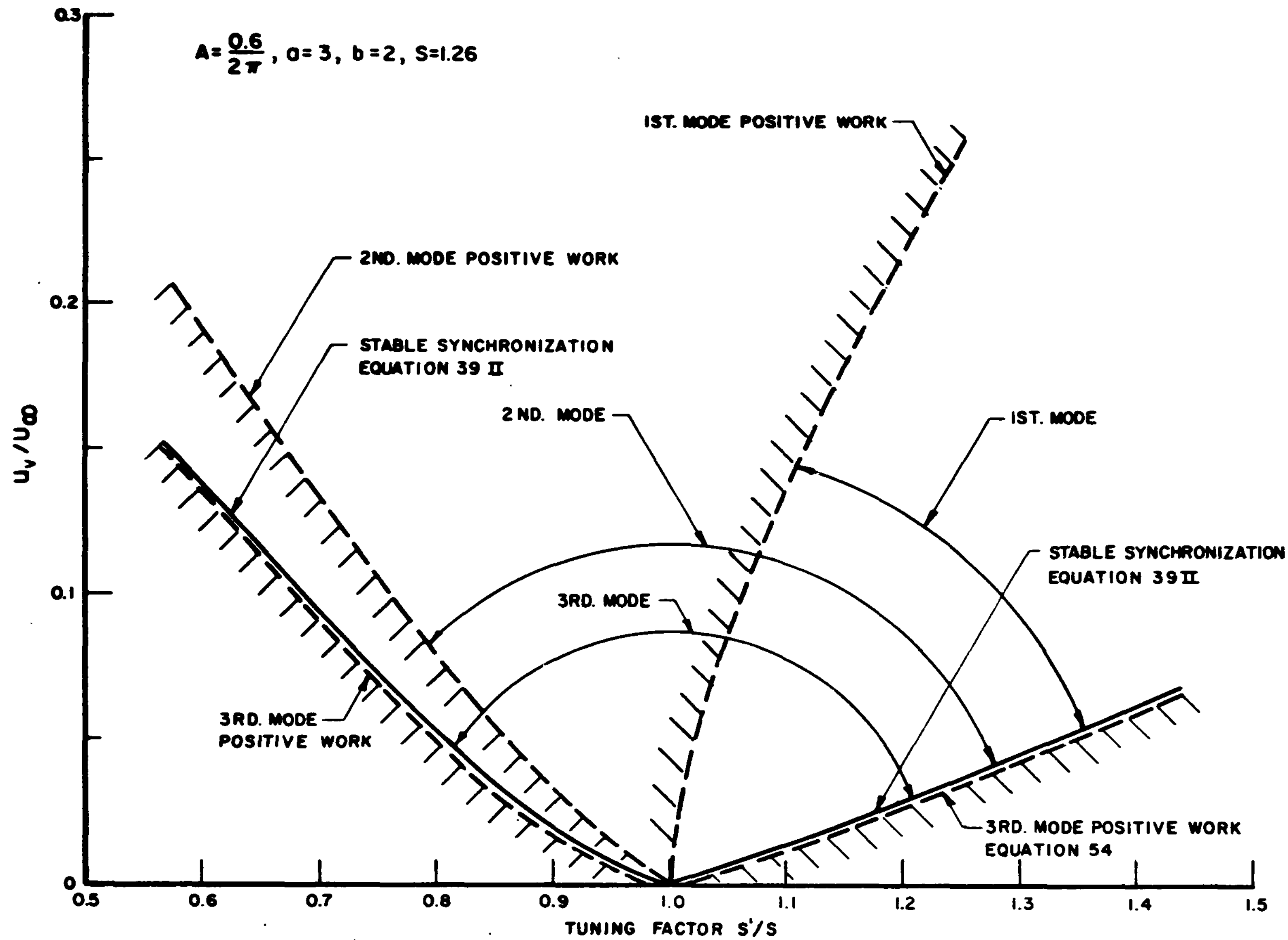

FIGURE 10c. EXISTENCE REGION OF SELF-EXCITED SINGING

R-1059

DISTRIBUTION LIST
Contract Nonr 263(52)

Copies

75 Commanding Officer and Director
DAVID TAYLOR MODEL BASIN
Washington, D. C. 20007
ATTN Code 513

10 Chief, BUREAU OF SHIPS
Department of the Navy
Washington 25, D. C.
ATTN:
Tech. Inf. Bur. (Code 210L) (3)
Ship Des. (Code 410) (1)
Ship Sil. Br. (Code 345) (1)
Prelim. Des. (Code 420) (2)
Hull Des. (Code 440) (1)
Scien. & Res. (Code 442) (1)
Ship Res. Br. (Code 341B) (1)

5 CHIEF OF NAVAL RESEARCH
Department of the Navy
Washington 25, D. C.
ATTN Code 438 (4)
Code 466 (1)

1 Commanding Officer
OFFICE OF NAVAL RESEARCH
495 Summer Street
Boston 10, Massachusetts

1 Commanding Officer
OFFICE OF NAVAL RESEARCH
1030 East Green Street
Pasadena 1, California

1 Commanding Officer
OFFICE OF NAVAL RESEARCH
219 South Dearborn Street
Chicago, Illinois 60601

1 Commanding Officer
OFFICE OF NAVAL RESEARCH
207 West 24th Street
New York 11, New York

Copies

15 Commanding Officer
OFFICE OF NAVAL RESEARCH
Navy 100, Box 39
Fleet Post Office
New York, New York

1 Commanding Officer
OFFICE OF NAVAL RESEARCH
1000 Geary Street
San Francisco 9, California

1 Chief, BUREAU OF WEAPONS
Department of the Navy
Washington 25, D. C.

20 DEFENSE DOCUMENTATION CENTER
Cameron Station, Bldg. 5
5010 Duke Street
Alexandria, Virginia 22314

1 Office of Ship Construction
MARITIME ADMINISTRATION
Department of Commerce
Washington 25, D. C.
ATTN V. L. Russo

1 Main Propulsion Section
Engineering Specification Branch
MARITIME ADMINISTRATION
Department of Commerce
Washington 25, D. C.
ATTN Caesar Tangerini

2 Commander
U. S. NAVAL ORDNANCE LABORATORY
White Oak
Silver Spring, Maryland
ATTN Library

3 Commander
U. S. NAVAL ORDNANCE TEST STATION
3202 East Foothill Boulevard
Pasadena, California
ATTN Tech. Lib. (1)
Head, Thrust Prod. Sec. (1)

DISTRIBUTION LIST (Contd.)
Contract 263(52)

Copies	
1	Commander U. S. NAVAL ORDNANCE TEST STATION 3202 East Foothill Boulevard Pasadena 8, California ATTN Code P-508
1	Director U. S. NAVAL RESEARCH LABORATORY Washington 25, D. C. Code 2000
1	BETHLEHEM STEEL COMPANY Shipbuilding Division 25 Broadway New York, New York ATTN Hollinshead De Luce Ass't to Vice President
1	Director, Hydrodynamics Laboratory CALIFORNIA INSTITUTE OF TECHNOLOGY Pasadena 4, California
1	DOUGLAS AIRCRAFT COMPANY, INC. Aircraft Division Long Beach, California ATTN J. Hess
1	Editor, ENGINEERING INDEX, INC. 345 East 47th Street New York, New York
1	GENERAL APPLIED SCIENCE LABORATORIES, INC. Merrick & Stewart Avenues Westbury, L. I., New York
2	GIBBS AND COX, INC. 21 West Street New York 6, New York ATTN W. F. Gibbs W. Bachman
1	HYDRONAUTICS, INC. Pindell School Road Laurel, Howard County, Maryland ATTN P. Eisenberg, President

Copies	
1	Librarian INSTITUTE OF AEROSPACE SCIENCES, INC. 2 East 64th Street New York 21, New York
1	ITEK CORPORATION Vidya Division 1450 Page Mill Road Palo Alto, California ATTN A. R. Kriebel
1	Capt. E. S. Arentzen, USN Commanding Officer U. S. Naval Reserve Officers Training Corps MASSACHUSETTS INSTITUTE OF TECHNOLOGY Cambridge 39, Massachusetts
2	Department of Civil Engineering MASSACHUSETTS INSTITUTE OF TECHNOLOGY Cambridge 39, Massachusetts
2	MASSACHUSETTS INSTITUTE OF TECHNOLOGY Department of Naval Architecture and Marine Engineering Cambridge 39, Massachusetts ATTN J. E. Kerwin F. M. Lewis
1	Mr. John Kane Engineering Technical Department NEWPORT NEWS SHIPBUILDING AND DRYDOCK COMPANY Newport News, Virginia
2	Director Ordnance Research Laboratory PENNSYLVANIA STATE UNIVERSITY P. O. Box 30 University Park, Pennsylvania
1	REED RESEARCH, INC. 1048 Potomac Street, N.W. Washington 7, D. C. ATTN S. Reed

DISTRIBUTION LIST (Contd.)
Contract 263(52)

Copies		Copies	
1	Librarian SOCIETY OF NAVAL ARCHITECTS AND MARINE ENGINEERS 74 Trinity Place New York, New York		
1	Editor Applied Mechanics Review SOUTHWEST RESEARCH INSTITUTE 8500 Culebra Road San Antonio 6, Texas		
1	TECHNICAL RESEARCH GROUP, INC. Route 110 Melville, New York 11749 ATTN J. Lurye		
2	Institute of Engineering Research UNIVERSITY OF CALIFORNIA Berkeley 4, California ATTN J. A. Schade J. V. Wehausen		
1	Department of Naval Architecture and Marine Engineering UNIVERSITY OF MICHIGAN Ann Arbor, Michigan ATTN R. B. Couch		
1	Director St. Anthony Falls Laboratory UNIVERSITY OF MINNESOTA Minneapolis, Minnesota		
2	Administrator WEBB INSTITUTE OF NAVAL ARCHITECTURE Glen Cove, New York ATTN Post Graduate School for Officers		
1	Department of Engineering Mechanics UNIVERSITY OF NOTRE DAME Notre Dame, Indiana 46556 ATTN A. G. Strandhagen		

UNCLASSIFIED
Security Classification

DOCUMENT CONTROL DATA - R&D

(Security classification of title, body of abstract and indexing annotation must be entered when the overall report is classified)

1. ORIGINATING ACTIVITY *(Corporate author)* DAVIDSON LABORATORY, Stevens Institute of Technology	2a. REPORT SECURITY CLASSIFICATION Unclassified 2b. GROUP

3. REPORT TITLE

AN ASPECT OF THE PROPELLER-SINGING PHENOMENON AS A SELF-EXCITED OSCILLATION

4. DESCRIPTIVE NOTES *(Type of report and inclusive dates)*

Final

5. AUTHOR(S) *(Last name, first name, initial)*

Shioiri, Jumpei

6. REPORT DATE	7a. TOTAL NO. OF PAGES	7b. NO. OF REFS
March 1965	35	8

8a. CONTRACT OR GRANT NO. Nonr 263(52) b. PROJECT NO. c. d.	9a. ORIGINATOR'S REPORT NUMBER(S) R-1059 9b. OTHER REPORT NO(S) *(Any other numbers that may be assigned this report)*

10. AVAILABILITY/LIMITATION NOTICES

Application for copies may be made to the Defense Documentation Center, Cameron Station, 5010 Duke Street, Alexandria, Virginia 22314.

11. SUPPLEMENTARY NOTES	12. SPONSORING MILITARY ACTIVITY Bureau of Ships General Hydrodynamics Research Program (S-R009-01-01) Administered by David Taylor Model Basin

13. ABSTRACT

A model for the propeller-singing phenomenon considered as a self-excited oscillation is presented to interpret the finding of a recent experimental work; viz., that, although the singing frequency roughly obeys the well-known Strouhal relation, once the strong singing state has been established, the frequency is kept constant through a fairly wide range of flow velocity, and consequently the frequency-versus-velocity diagram exhibits step and jump characteristics. The model presented is a "closed loop" composed of a blade, as a mechanical-vibration system, and the Kármán vortex-shedding mechanism; the blade vibration controls the shedding mechanism, and the hydrodynamic reaction of shed vortices sustains the blade vibration. The control imposed by the blade vibration upon the vortex shedding actually implies the synchronization of the latter with the former. The model which simulates the vortex-shedding mechanism is essentially a simplified mathematical expression for the disintegration process of the vortex sheets shed from the separation points into the rows of discrete vortices. The stability criterion derived for the synchronized run of the shedding mechanism, together with the positive-work criterion imposed upon the phase relation between the blade vibration and the hydrodynamic reaction of the shed vortices, gives a reasonable interpretation for the step and jump characteristics.

DD FORM 1 JAN 64 1473

UNCLASSIFIED
Security Classification

14. KEY WORDS	LINK A		LINK B		LINK C	
	ROLE	WT	ROLE	WT	ROLE	WT
Propeller-Singing						

INSTRUCTIONS

1. ORIGINATING ACTIVITY: Enter the name and address of the contractor, subcontractor, grantee, Department of Defense activity or other organization *(corporate author)* issuing the report.

2*a*. REPORT SECURITY CLASSIFICATION: Enter the overall security classification of the report. Indicate whether "Restricted Data" is included. Marking is to be in accordance with appropriate security regulations.

2*b*. GROUP: Automatic downgrading is specified in DoD Directive 5200.10 and Armed Forces Industrial Manual. Enter the group number. Also, when applicable, show that optional markings have been used for Group 3 and Group 4 as authorized.

3. REPORT TITLE: Enter the complete report title in all capital letters. Titles in all cases should be unclassified. If a meaningful title cannot be selected without classification, show title classification in all capitals in parenthesis immediately following the title.

4. DESCRIPTIVE NOTES: If appropriate, enter the type of report, e.g., interim, progress, summary, annual, or final. Give the inclusive dates when a specific reporting period is covered.

5. AUTHOR(S): Enter the name(s) of author(s) as shown on or in the report. Enter last name, first name, middle initial. If military, show rank and branch of service. The name of the principal author is an absolute minimum requirement.

6. REPORT DATE: Enter the date of the report as day, month, year; or month, year. If more than one date appears on the report, use date of publication.

7*a*. TOTAL NUMBER OF PAGES: The total page count should follow normal pagination procedures, i.e., enter the number of pages containing information.

7*b*. NUMBER OF REFERENCES: Enter the total number of references cited in the report.

8*a*. CONTRACT OR GRANT NUMBER: If appropriate, enter the applicable number of the contract or grant under which the report was written.

8*b*, 8*c*, & 8*d*. PROJECT NUMBER: Enter the appropriate military department identification, such as project number, subproject number, system numbers, task number, etc.

9*a*. ORIGINATOR'S REPORT NUMBER(S): Enter the official report number by which the document will be identified and controlled by the originating activity. This number must be unique to this report.

9*b*. OTHER REPORT NUMBER(S): If the report has been assigned any other report numbers *(either by the originator or by the sponsor)*, also enter this number(s).

10. AVAILABILITY/LIMITATION NOTICES: Enter any limitations on further dissemination of the report, other than those imposed by security classification, using standard statements such as:

(1) "Qualified requesters may obtain copies of this report from DDC."

(2) "Foreign announcement and dissemination of this report by DDC is not authorized."

(3) "U. S. Government agencies may obtain copies of this report directly from DDC. Other qualified DDC users shall request through
______________________________."

(4) "U. S. military agencies may obtain copies of this report directly from DDC. Other qualified users shall request through
______________________________."

(5) "All distribution of this report is controlled. Qualified DDC users shall request through
______________________________."

If the report has been furnished to the Office of Technical Services, Department of Commerce, for sale to the public, indicate this fact and enter the price, if known.

11. SUPPLEMENTARY NOTES: Use for additional explanatory notes.

12. SPONSORING MILITARY ACTIVITY: Enter the name of the departmental project office or laboratory sponsoring *(paying for)* the research and development. Include address.

13. ABSTRACT: Enter an abstract giving a brief and factual summary of the document indicative of the report, even though it may also appear elsewhere in the body of the technical report. If additional space is required, a continuation sheet shall be attached.

It is highly desirable that the abstract of classified reports be unclassified. Each paragraph of the abstract shall end with an indication of the military security classification of the information in the paragraph, represented as *(TS)*, *(S)*, *(C)*, or *(U)*.

There is no limitation on the length of the abstract. However, the suggested length is from 150 to 225 words.

14. KEY WORDS: Key words are technically meaningful terms or short phrases that characterize a report and may be used as index entries for cataloging the report. Key words must be selected so that no security classification is required. Identifiers, such as equipment model designation, trade name, military project code name, geographic location, may be used as key words but will be followed by an indication of technical context. The assignment of links, roles, and weights is optional.

DAVIDSON LABORATORY Report 1059 (Unclassified) March 1965

AN ASPECT OF THE PROPELLER-SINGING PHENOMENON AS A SELF-EXCITED OSCILLATION

By Jumpei Shioiri

BuShips Fundamental Hydromechanics Research Program (S-R009-01-01) Administered by DTMB, Contract Nonr 263(52), (DL Project 2661/056)

A model for the propeller-singing phenomenon considered as a self-excited oscillation is presented to interpret the finding of a recent experimental work; viz., that, although the singing frequency roughly obeys the well-known Strouhal relation once the strong singing state has been established, the frequency is kept constant through a fairly wide range of flow velocity, and consequently the frequency-versus-velocity diagram exhibits step and jump characteristics. The model presented is a "closed loop" composed of a blade, as a mechanical-vibration system, and the Kármán vortex-shedding mechanism; the blade vibration controls the shedding mechanism, and the hydrodynamic reaction of shed vortices sustains the blade vibration. The control imposed by the blade vibration upon the vortex shedding actually implies the synchronization of the latter with the former. The model which simulates the vortex shedding

DAVIDSON LABORATORY Report 1059 (Unclassified) March 1965

AN ASPECT OF THE PROPELLER-SINGING PHENOMENON AS A SELF-EXCITED OSCILLATION

By Jumpei Shioiri

BuShips Fundamental Hydromechanics Research Program (S-R009-01-01) Administered by DTMB, Contract Nonr 263(52), (DL Project 2661/056)

A model for the propeller-singing phenomenon considered as a self-excited oscillation is presented to interpret the finding of a recent experimental work; viz., that, although the singing frequency roughly obeys the well-known Strouhal relation once the strong singing state has been established, the frequency is kept constant through a fairly wide range of flow velocity, and consequently the frequency-versus-velocity diagram exhibits step and jump characteristics. The model presented is a "closed loop" composed of a blade, as a mechanical-vibration system, and the Kármán vortex-shedding mechanism; the blade vibration controls the shedding mechanism, and the hydrodynamic reaction of shed vortices sustains the blade vibration. The control imposed by the blade vibration upon the vortex shedding actually implies the synchronization of the latter with the former. The model which simulates the vortex shedding

DAVIDSON LABORATORY Report 1059 (Unclassified) March 1965

AN ASPECT OF THE PROPELLER-SINGING PHENOMENON AS A SELF-EXCITED OSCILLATION

By Jumpei Shioiri

BuShips Fundamental Hydromechanics Research Program (S-R009-01-01) Administered by DTMB, Contract Nonr 263(52), (DL Project 2661/056)

A model for the propeller-singing phenomenon considered as a self-excited oscillation is presented to interpret the finding of a recent experimental work; viz., that, although the singing frequency roughly obeys the well-known Strouhal relation once the strong singing state has been established, the frequency is kept constant through a fairly wide range of flow velocity, and consequently the frequency-versus-velocity diagram exhibits step and jump characteristics. The model presented is a "closed loop" composed of a blade, as a mechanical-vibration system, and the Kármán vortex-shedding mechanism; the blade vibration controls the shedding mechanism, and the hydrodynamic reaction of shed vortices sustains the blade vibration. The control imposed by the blade vibration upon the vortex shedding actually implies the synchronization of the latter with the former. The model which simulates the vortex-shedding

DAVIDSON LABORATORY Report 1059 (Unclassified) March 1965

AN ASPECT OF THE PROPELLER-SINGING PHENOMENON AS A SELF-EXCITED OSCILLATION

By Jumpei Shioiri

BuShips Fundamental Hydromechanics Research Program (S-R009-01-01) Administered by DTMB, Contract Nonr 263(52), (DL Project 2661/056)

A model for the propeller-singing phenomenon considered as a self-excited oscillation is presented to interpret the finding of a recent experimental work; viz., that, although the singing frequency roughly obeys the well-known Strouhal relation once the strong singing state has been established, the frequency is kept constant through a fairly wide range of flow velocity, and consequently the frequency-versus-velocity diagram exhibits step and jump characteristics. The model presented is a "closed loop" composed of a blade, as a mechanical-vibration system, and the Kármán vortex-shedding mechanism; the blade vibration controls the shedding mechanism, and the hydrodynamic reaction of shed vortices sustains the blade vibration. The control imposed by the blade vibration upon the vortex shedding actually implies the synchronization of the latter with the former. The model which simulates the vortex-shedding

mechanism is essentially a simplified mathematical expression for the disintegration process of the vortex sheets shed from the separation points into the rows of discrete vortices. The stability criterion derived for the synchronized run of the shedding mechanism, together with the positive-work criterion imposed upon the phase relation between the blade vibration and the hydrodynamic reaction of the shed vortices, gives a reasonable interpretation for the step and jump characteristics.

KEYWORD

Propeller-Singing

mechanism is essentially a simplified mathematical expression for the disintegration process of the vortex sheets shed from the separation points into the rows of discrete vortices. The stability criterion derived for the synchronized run of the shedding mechanism, together with the positive-work criterion imposed upon the phase relation between the blade vibration and the hydrodynamic reaction of the shed vortices, gives a reasonable interpretation for the step and jump characteristics.

KEYWORD

Propeller-Singing

mechanism is essentially a simplified mathematical expression for the disintegration process of the vortex sheets shed from the separation points into the rows of discrete vortices. The stability criterion derived for the synchronized run of the shedding mechanism, together with the positive-work criterion imposed upon the phase relation between the blade vibration and the hydrodynamic relation of the shed vortices, gives a reasonable interpretation for the step and jump characteristics.

KEYWORD

Propeller-Singing

mechanism is essentially a simplified mathematical expression for the disintegration process of the vortex sheets shed from the separation points into the rows of discrete vortices. The stability criterion derived for the synchronized run of the shedding mechanism, together with the positive-work cirterion imposed upon the phase relation between the blade vibration and the hydrodynamic reaction of the shed vortices, gives a reasonable interpretation for the step and jump characteristics.

KEYWORD

Propeller-Singing